

AEDC-TR-69-25

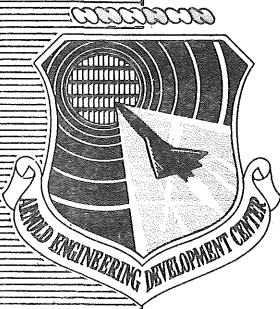
FEB 12 1969

MAR 5 1969

JAN 27 1971

JUL 6 1971

cy 2



DEVELOPMENT OF THERMOCOUPLE-TYPE TOTAL TEMPERATURE PROBES IN THE HYPERSONIC FLOW REGIME

P. J. Bontrager

ARO, Inc.

January 1969

This document has been approved for public release
and sale; its distribution is unlimited.

**VON KÁRMÁN GAS DYNAMICS FACILITY
ARNOLD ENGINEERING DEVELOPMENT CENTER
AIR FORCE SYSTEMS COMMAND
ARNOLD AIR FORCE STATION, TENNESSEE**

PROPERTY OF U. S. AIR FORCE
AEDC LIBRARY
F40600-69-C-0001

DEVELOPMENT OF THERMOCOUPLE-TYPE
TOTAL TEMPERATURE PROBES IN THE
HYPERSONIC FLOW REGIME

P. J. Bontrager
ARO, Inc.

This document has been approved for public release
and sale; its distribution is unlimited.

FOREWORD

The work reported herein was done at the request of the Arnold Engineering Development Center (AEDC), Air Force Systems Command (AFSC), under Program Element 65401F, Project 876A, Task G226.

The results of tests presented were obtained by ARO, Inc. (a subsidiary of Sverdrup & Parcel and Associates, Inc.), contract operator of the AEDC, Arnold Air Force Station, Tennessee, under Contract F40600-69-C-0001. These tests were conducted during the period from September 1966 to February 1968, under ARO Project Nos. VT2715, VT8002, and VT2806, and the manuscript was submitted for publication on December 20, 1968.

The contents of this report were submitted to the University of Tennessee Space Institute as partial fulfillment of the requirements for a Master of Science degree.

The author wishes to acknowledge the many persons in the von Karman Gas Dynamics Facility, Arnold Engineering Development Center, whose assistance was instrumental in the conduction of the experimental work and in the preparation of this thesis. The author is particularly indebted to Mr. J. C. Sivells, Mr. H. T. Wood, and Mr. H. W. Ball of ARO, Inc. and the Arnold Engineering Development Center, U. S. Air Force, for their permission to use the experimental work as material for the thesis. Thanks are also due Dr. W. Frost for his assistance in the preparation and review of the thesis.

This technical report has been reviewed and is approved.

Eugene C. Fletcher
Lt Col, USAF
AF Representative, VKF
Directorate of Test

Roy R. Croy, Jr.
Colonel, USAF
Director of Test

ABSTRACT

An experimental study to develop the criterion necessary to construct a miniature shielded thermocouple total temperature probe suitable for application in the hypersonic flow regime. Particular emphasis was given to the effect that internal velocity and thermocouple junction location relative to the shield entrance had on temperature measurements. An error analysis resulting from heat transfer phenomenon was made. The measured total temperature-to-tunnel stilling chamber temperature ratio was correlated in terms of the entrance flow length-to-probe length ratio. Over the range of parameters investigated both the optimum length-to-diameter and the optimum entrance-to-vent area ratios were found to be two. The entrance flow length-to-probe length ratios effectively correlated the data from probes of a given internal diameter.

TABLE OF CONTENTS

CHAPTER	PAGE
I. INTRODUCTION	1
II. EXPERIMENTAL REVIEW	3
III. APPARATUS	6
Wind Tunnel	6
Hypersonic Wind Tunnels B and C	6
Hypersonic Wind Tunnel E	8
Probes	8
Instrumentation	12
IV. TEST CONDITIONS AND PROCEDURE	15
V. ERROR ANALYSIS	20
Velocity Error	20
Conduction Error	21
Radiation Error	23
VI. THEORETICAL CONSIDERATIONS	29
VII. RESULTS AND DISCUSSION	31
VIII. CONCLUSIONS	56
BIBLIOGRAPHY	57

LIST OF TABLES

TABLE	PAGE
I. Probe Dimensions	11
II. Test Conditions	16
III. Probe Length-to-Diameter Ratio	17
IV. Probe Entrance-to-Vent Area Ratio	18
V. Error for A 0.144-inch Internal Diameter Probe	38

LIST OF FIGURES

FIGURE	PAGE
1. Tunnel C	7
2. Tunnel E	9
3. Probe Geometry	10
4. Typical Probe Installation (Tunnel C)	13
5. Per cent Velocity Error as a Function of Mach Number . . .	22
6. Conduction Error as a Function of Reynolds Number	24
7. Configuration Factor	25
8. Per cent Radiation Error as a Function of Reynolds Number	27
9. Effect of Stagnation Pressure on Measured Temperature Ratio at Various Length-to-Diameter Ratios for 0.150- inch Internal Diameter Probes	32
10. Effect of Stagnation Pressure on Measured Temperature Ratio at Various Length-to-Diameter Ratios	34
11. Effect of Length-to-Diameter Ratio on Measured Temperature Ratio	36
12. Effect of Stagnation Pressure on Measured Temperature Ratio at Various Entrance-to-Vent Area Ratios	39
13. Effect of Stagnation Pressure on Measured Temperature Ratio at Various Entrance-to-Vent Area Ratios for 0.144-inch Internal Diameter Probes	41

FIGURE	PAGE
14. Effect of Stagnation Pressure on Measured Temperature Ratio at Various Entrance-to-Vent Area Ratios for 0.076- inch Internal Diameter Probes	42
15. Effect of Stagnation Pressure on Measured Temperature Ratio at Various Entrance-to-Vent Area Ratios for 0.056- inch Internal Diameter Probes	43
16. Effect of Entrance Area-to-Vent Area Ratio on Measured Temperature Ratio at Various Length-to-Diameter Ratios for 0.144-inch Internal Diameter Probes	44
17. Effect of Entrance Area-to-Vent Area Ratio on Measured Temperature Ratio at Various Length-to-Diameter Ratios for 0.076-inch Internal Diameter Probes	46
18. Effect of Radiation Shields on Measured Temperature Ratios	47
19. Effect of Stagnation Pressure and Temperature on Measured Temperature Ratios at a Constant Free-Stream Reynolds Number of $0.5 \times 10^6 \text{ ft}^{-1}$	48
20. Temperature Ratio as a Function of L_e/L for Probes of 0.144- and 0.150-inch Internal Diameter	49
21. Temperature Ratio as a Function of L_e/L for Probes of 0.056- and 0.076-inch Internal Diameter	50
22. Temperature Ratio as a Function of L_e/L for 0.020-inch Internal Diameter Probes	51
23. Summary of Correlation Data	53

NOMENCLATURE

A	Cross-sectional area, ft^2
a	Speed of sound, ft/sec
C_p	Specific heat capacity of gas at constant pressure, $\text{Btu}/\text{lb}_m\text{-}^\circ\text{R}$
D	Probe internal diameter, ft (unless otherwise noted)
d	Thermocouple wire diameter, ft
E_c	Conduction error, $^\circ\text{R}$
E_r	Radiation error, $^\circ\text{R}$
E_v	Velocity error, $^\circ\text{R}$
F_{ji}	Configuration factor for radiation from the thermocouple junction to Zone i of the enclosure
g	Gravitational conversion factor, $\text{lb}_m\text{-ft}/\text{lb}_f\text{-sec}^2$
h	Convective heat transfer coefficient, $\text{Btu}/\text{ft}^2\text{-hr-}^\circ\text{R}$
J	Mechanical equivalent of heat, $\text{ft-lb}_f/\text{Btu}$ (778)
k	Thermal conductivity, $\text{Btu}/\text{ft-hr-}^\circ\text{R}$
L	Probe length, distance from entrance to thermocouple junction (see Figure 3), ft (unless otherwise noted)
L_e	Length of region of underdeveloped flow in probe, ft
l	Exposed length of thermocouple wire, ft
M	Mach number
p	Pressure, lb_f/ft^2 (unless otherwise noted)
R	Gas constant, $1716.3 \text{ ft}^2/\text{sec}^2\text{-}^\circ\text{R}$
Re	Unit Reynolds number, ft^{-1}

T	Temperature, °R
T _e	Effective temperature, °R
T _i	Temperature of the i th Zone of the enclosure, °R
u	Velocity, ft/sec
α	Recovery factor, Equation 1
γ	Ratio of specific heat, 1.4
ε	Emittance of thermocouple material
μ	Viscosity, slug/ft-sec
ρ	Density, slug/ft ³
σ	Stefan-Boltzman constant, 1.714 x 10 ⁻⁹ Btu/ft ² -hr-°R ⁴
ω	Mass flow, slug/sec
Δω	An element of solid angle, steradian

Subscripts

D	Reynolds number based upon probe internal diameter
d	Reynolds number based upon thermocouple wire diameter
e	Probe entrance conditions
j	Probe junction conditions
o	Tunnel stilling chamber conditions
s	Gas stream static conditions
sp	Thermocouple support conditions
w	Thermocouple wire conditions
v	Probe vent conditions
∞	Gas free stream conditions

CHAPTER I

INTRODUCTION

Measurements of the total temperature of air flowing at hypersonic Mach numbers present special difficulties because of the heat of compression and the heat of friction involved in the gas while it is flowing to the measuring device. Today, high-velocity flow total temperature measurements have become increasingly important in engineering technology and sufficiently accurate methods of measuring total temperature are therefore urgently needed. This is especially true in measuring total temperature in high-velocity low density wind tunnels and also in measuring temperature profiles in boundary layers.

To measure total temperature the gas is brought nearly to rest in a temperature probe and then the low-velocity gas stream is measured by a thermocouple. A discussion of the factors involved in the design of a total temperature probe can be found in a paper by Hottel and Kalitinsky (1)¹. Numerous attempts have been made to develop temperature probes in the subsonic and supersonic flow regime to measure the temperature which the gas assumes in a state of stagnation after an adiabatic temperature rise (2 through 18). However, from experience of total temperature measurements in the von Karman

¹Numbers in parentheses refer to similarly numbered references in the bibliography.

Gas Dynamics Facility (VKF) Hypersonic wind tunnels, using probes designed from the recommended criterion for subsonic and supersonic flow regime, the probes gave erroneous measurements. This may be accounted for by the fact that in the VKF Hypersonic tunnel the Reynolds number range inside the probe is lower than in the subsonic or supersonic regime investigated in References 2 through 18.

The purpose of the present work is to develop the criterion necessary to construct a miniature shielded total temperature probe suitable for application in hypersonic wind tunnels. Particular emphasis will be given to the effect that internal velocity and thermocouple junction location has on temperature measurements.

Experiments were carried out with probe internal diameters ranging from 0.020 to 0.150 inch. The large probes were used initially because it was easier to make probe geometry changes.

Analysis of the errors resulting from heat transfer phenomenon is made and it is shown that the main source of error is radiation losses to the cold tunnel walls.

CHAPTER II

EXPERIMENTAL REVIEW

The purpose of this chapter is to review the experimental investigation on total temperature probes reported in the literature. The main area of interest in the literature has been to investigate the effect of internal velocity and the effect of exposed thermocouple wire length on temperature measurements. These investigations have been conducted over a large range of Reynolds numbers, Mach numbers, and temperatures. At present, no one has investigated probes in the hypersonic flow regime nor has anyone developed a probe diminutive enough to be used for total temperature measurements in boundary layer.

Successful measurements of total temperature have been obtained for flow at low velocity and low temperature with a probe as reported in References 2, 3, 4, 5, and 6. These papers include results from tests of both shielded and unshielded probes. For supersonic flow, Goldstein and Scherrer (7) found that for a free stream Mach number of 1.50 and a total temperature of 520°R the optimum ratio of vent area-to-entrance area was 0.500 to 0.625 and the total temperature probe is insensitive to angle of inclination up to 9 degrees. Werner, Keppel, and Bernards (8,9) investigated the effects on temperature measurements of the number of radiation shields and the effect of internal velocity over a free stream Mach number range of 0.80 to 5.0 and a temperature

up to 2000°R. They showed that only in a special application would it be profitable to increase the number of shields over three. It was also found that the optimum internal Mach numbers were 0.20 within the inner-shield and 0.30 between the inner- and outer-shield.

Winkler (10,11) investigated the effects of vent area-to-entrance area ratios and the length of the thermocouple wire projection over a Mach number range of 4.90 to 7.60 and a temperature range up to 720°R. The optimum vent-to-entrance area ratio was found to be 0.20 over the range investigated. It was also shown that two vent holes spaced 180 degrees apart were better than just one vent hole. Werner, Keppel and Huppert (12,13) developed large total temperature probes for flight use up to 8000 feet altitude and up to a Mach number of 3.0. These probes are designed for operational use on service aircraft. Hagins (14) investigated and made an error analysis on total temperature probes to be used in a stilling chamber of a wind tunnel. This investigation was made at low velocity and for temperatures as high as 2200°R. The investigation studied the effects of radiation shields and the influence of the angle between the shield and the flow direction on temperature measurements.

Other methods for measuring total temperature have been attempted. Wood (15) used a probe with a heated shield and base to reduce conduction and radiation losses.

Warshawsky and Kuhns (16), Welshimer (17), and Lee (18) used a sonic pneumatic probe. The inability to calibrate these probes at the exact conditions where they will be used makes them impractical. The

accuracy of the sonic pneumatic probe depends upon the design and also the material used to construct the probe.

The foregoing investigations have been limited to low Mach numbers or low temperatures. The purpose of this study is (1) to determine why the criterion given for supersonic flow would not work in the hypersonic flow regime, (2) to develop the criterion necessary to construct a probe suitable for application in hypersonic wind tunnels, and (3) to provide experimental data on total temperature probes in the hypersonic flow regime at elevated temperatures. Emphasis will be given to the effects that internal velocity and thermocouple junction location have on temperature measurements. This investigation will also include probes of 0.020-inch internal diameter that can be used for temperature profile measurements in a boundary layer.

CHAPTER III

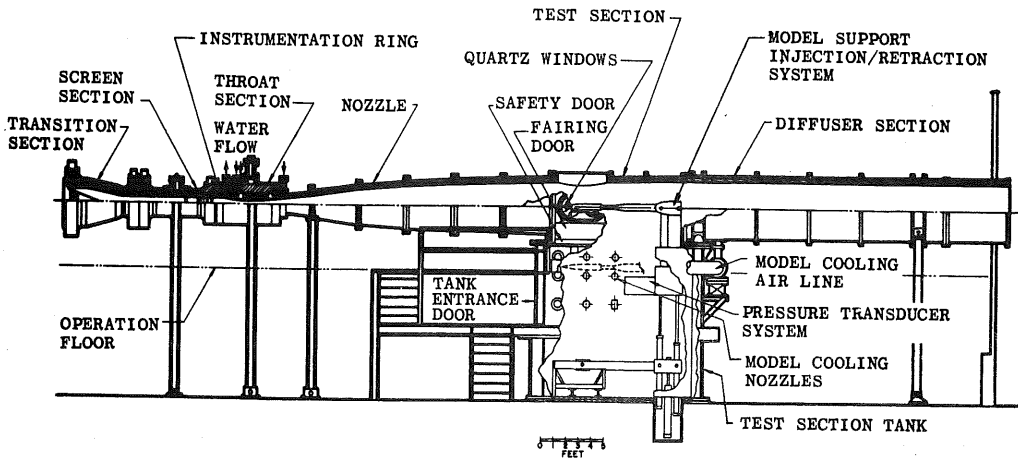
APPARATUS

I. WIND TUNNEL

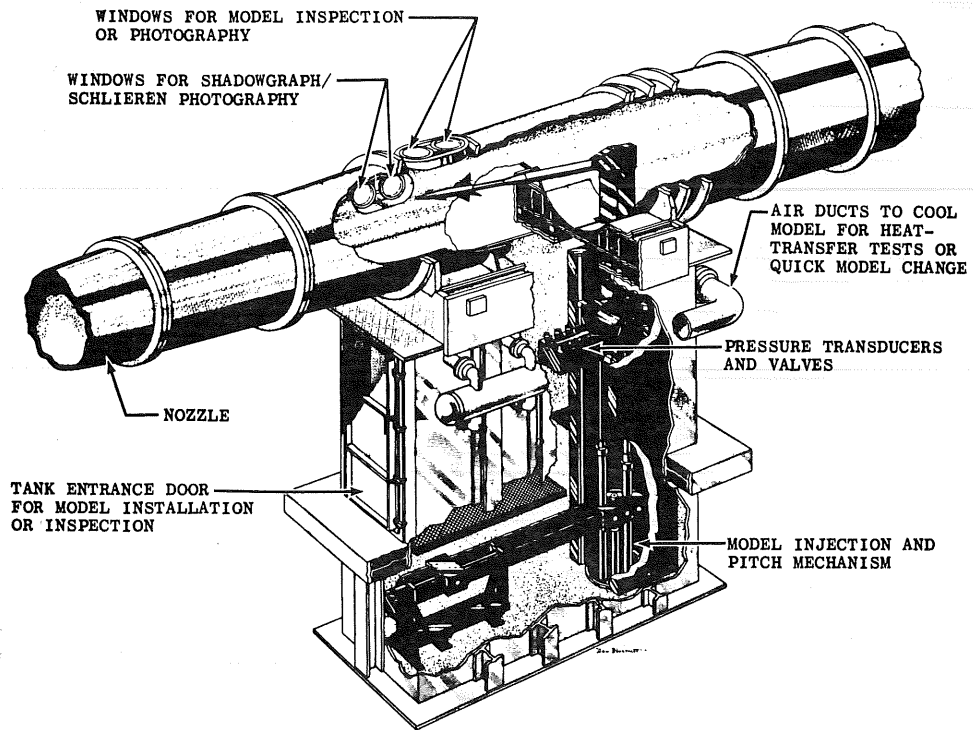
The experimental data reported herein were obtained in three of the VKF Hypersonic Wind Tunnels:

1. Gas Dynamic Wind Tunnel, Hypersonic (B),
2. Gas Dynamic Wind Tunnel, Hypersonic (C), and
3. Gas Dynamic Wind Tunnel, Hypersonic (E).

Hypersonic Wind Tunnels B and C. Tunnels B and C are continuous, closed-circuit, variable density wind tunnels with axisymmetric contoured nozzles and 50-in.-diameter test sections. Tunnel B operates at a nominal Mach number of 6 and 8 and at stagnation pressures from 20 to 280 and from 50 to 900 pounds per square inch absolute (psia), respectively. Tunnel C operates at a nominal Mach number of 10 and 12 and at stagnation conditions from 200 to 2000 and 600 to 2000 psia, respectively. Stagnation temperatures up to 1350°R in Tunnel B and 2400°R in Tunnel C are utilized to prevent liquefaction of the air in the test section. The above operating conditions result in free-stream unit Reynolds numbers from 0.30×10^6 to 5.00×10^6 per foot in Tunnel B and from 0.30×10^6 to 2.35×10^6 per foot in Tunnel C. Tunnel C and its associated equipment are shown in Figure 1. Details of Tunnel B are similar to those of Tunnel C. The



a. Tunnel assembly



b. Tunnel test section

Fig. 1 Tunnel C

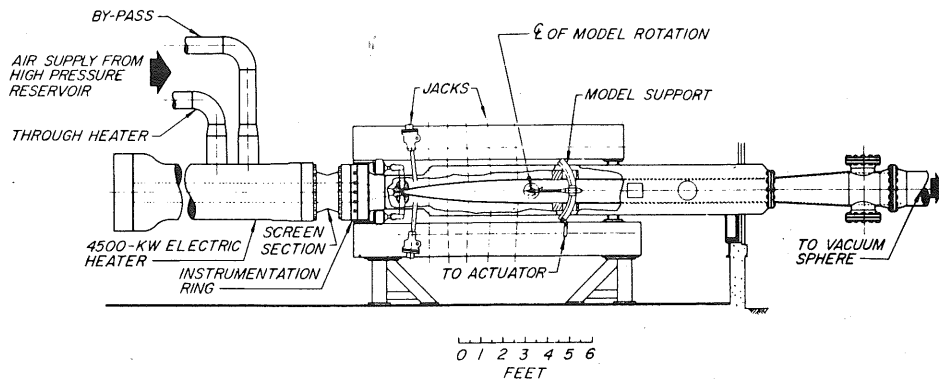
test section tank and safety doors allow the model to be injected into the test section for a test run and then retracted for model cooling or model changes without interrupting the tunnel flow.

Hypersonic Wind Tunnel E. Tunnel E, Figure 2, is an intermittent, variable density wind tunnel with a flexible plate-type nozzle and a 12-by-12-inch test section. The tunnel operates at Mach numbers from 5 to 8 at maximum stagnation pressures from 400 to 1600 psia, respectively, and stagnation temperatures up to 1400°R to prevent liquefaction. Minimum stagnation pressures are about one-quarter of the maximum at each Mach number. The above operating conditions result in maximum free-stream unit Reynolds numbers of 15.6×10^6 and 6.5×10^6 per foot and minimum free-stream unit Reynolds numbers of 4.8×10^6 and 2.0×10^6 per foot at Mach numbers 5 and 8, respectively.

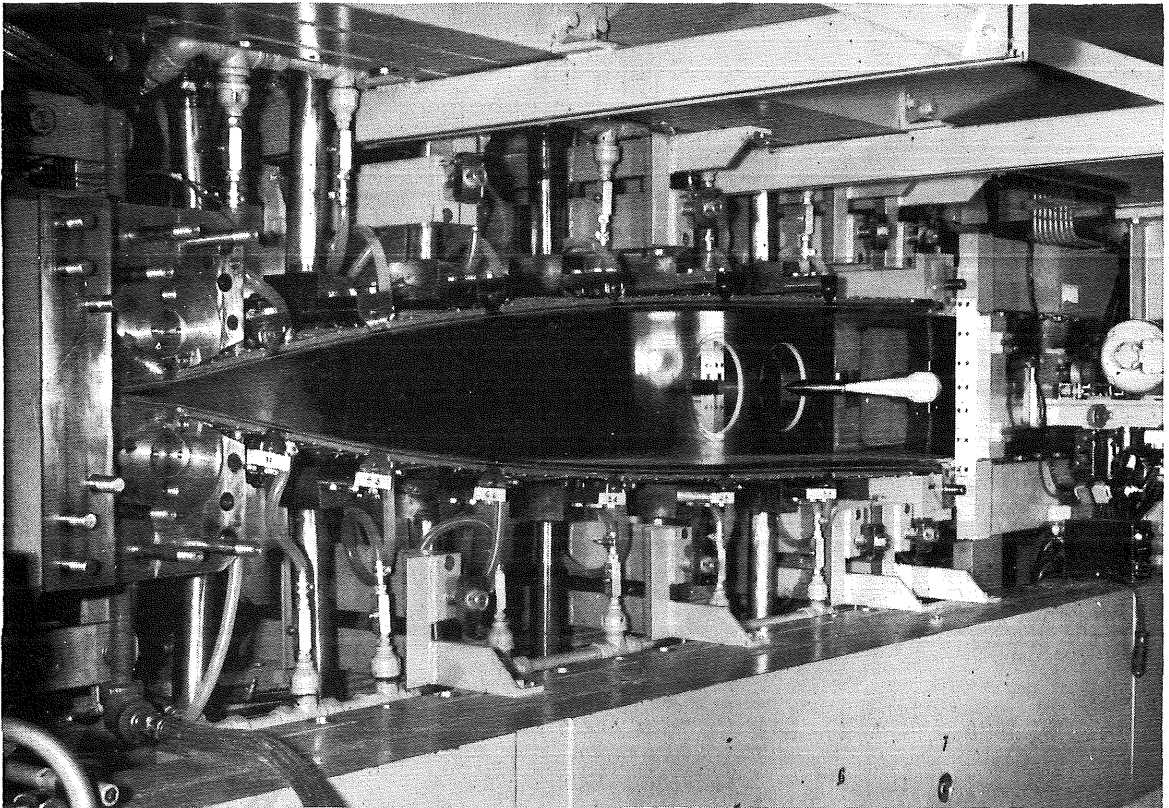
A more complete description of the Gas Dynamic Hypersonic Wind Tunnels may be found in Reference 19.

II. PROBES

Probe geometries are shown in Figure 3, page 10, and related probe dimensions are presented in Table I, page 11. All probes were constructed from Type 304 stainless steel tubing and with steel shrouded Chromel-Alumel thermocouple wire. All probes except the 0.150-inch internal diameter probes were constructed of standard thin wall stainless steel tubing. The 0.150-inch internal diameter probes were constructed from standard 0.144-inch internal diameter tubing

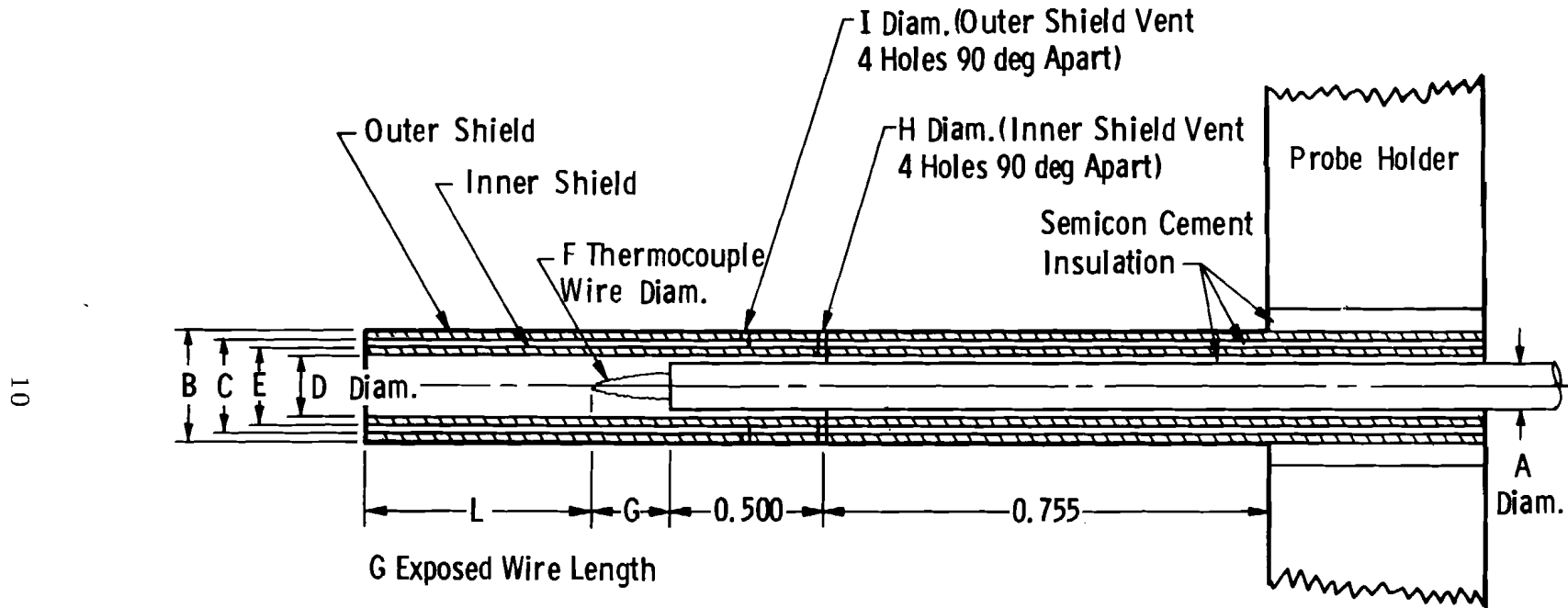


a. Tunnel assembly



b. Tunnel nozzle and test section

Fig. 2 Tunnel E



Note: All Dimensions in Inches and Typical Actual Probe Dimensions Given in Table I

Fig. 3 Probe Geometry

TABLE I
PROBE DIMENSIONS*

Probe I.D., in. D	A	B	C	E	F	G
0.150**	0.040	0.250	0.240	0.156	0.007	0.350
0.150	0.040	0.250	0.240	0.156	0.007	0.350
0.144	0.040	0.187	0.177	0.156	0.007	0.350
0.144	0.040	---	---	0.156	0.007	0.350
0.076	0.040	---	---	0.080	0.007	0.350
0.056	0.040	0.080	0.076	0.060	0.007	0.350
0.056	0.040	---	---	0.060	0.007	0.350
0.020	0.010	0.038	0.034	0.024	0.0015	0.075

Probe I.D., in. D	H	I	L	L/D	A_e/A_v	No. of Shields
0.150**	0.032	0.079	0.750	5	5.5	2
0.150	0.032-0.053	0.079	6.65-0.00	44.3-0.5	5-2.1	2, 1, 0
0.144	0.032	0.042	1.080-0.00	7.5-0	5.0	2, 1, 0
0.144	0.016-0.073	---	0.432-0.144	3,2,1	20-1	1
0.076	0.0085-0.0380	---	0.228-0.076	3,2,1	20-1	1
0.056	0.0125	0.021	0.280-0.056	5.0-1	5.0	2
0.056	0.0063-0.028	---	0.168-0.056	3,2,1	20-1	1
0.020	0.00446	0.009	0.100-0.020	5.0-1	5.0	2

*All dimensions in inches.

**Probe used as a standard during all tests.

and bored out to 0.150-inch. The tolerance on all internal diameters was ± 0.001 . The thermocouple wire was purchased enclosed in Type 304 stainless steel protective tubing with magnesium oxide (MgO) insulation between the two wires and also between the wires and protective tubing. Semicon cement was used as an insulator between the thermocouple protective tube and the inner radiation shield, between the radiation shields, and between the outer radiation shield and probe holder. A typical installation photograph of several probes in Tunnel C is shown in Figure 4.

A 0.150-inch internal diameter probe was used as a standard during all tunnel entries. The standard probe was constructed with an entrance-to-vent area ratio as recommended in Reference 11. The length of the exposed wire was 50 times the wire diameter to reduce conduction losses and the thermocouple junction was located five diameters inside the entrance of the probe.

III. INSTRUMENTATION

The Tunnel B and E stilling chamber temperatures were measured with one Chromel-Alumel thermocouple probe. The Tunnel C stilling chamber temperature was obtained from an electrical average¹ of the

¹By connecting thermocouples in parallel with equal wire resistance the thermocouple emfs will balance each other so that the emf output of the thermocouple network will be an electrical average. The temperature indicator is a null balance device and after balance presents an infinite impedance to the thermocouple network and as such does not influence the network emf.

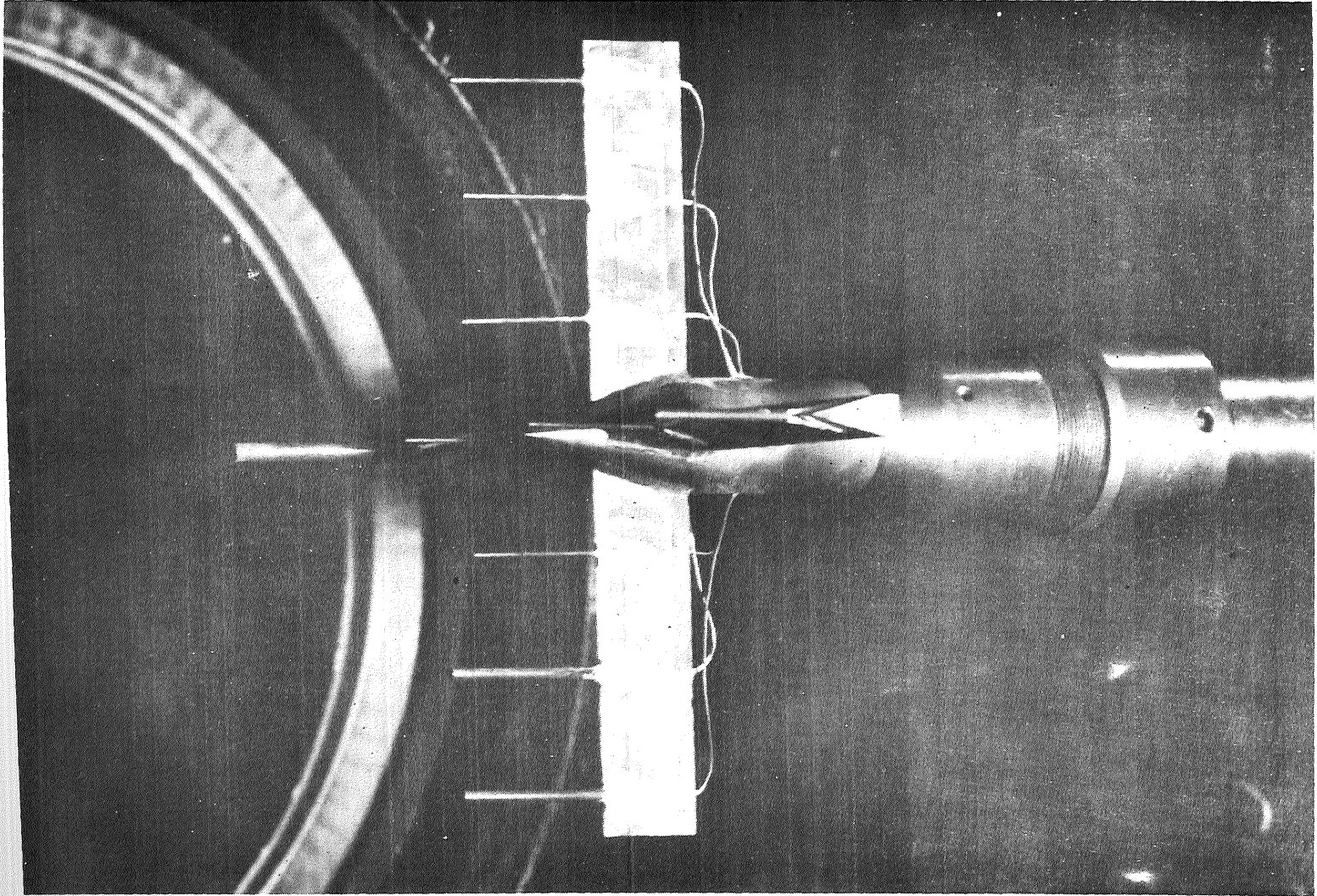


Fig. 4 Typical Probe Installation (Tunnel C)

readings of five Chromel-Alumel thermocouple probes. A pressure transducer was used to measure the wind tunnel stilling chamber pressure. All temperatures and pressures were monitored and the output digitized with a servopotentiometer, Leeds and Northrup Midget Model D. After analog-to-digital conversion of the measurements, data reduction was performed with a CDC 1604B digital computer. Based upon the thermocouple wire manufacturer's literature and a knowledge of the VKF temperature recording system, the estimated precision of the probe and stilling chamber temperature is 1 per cent.

CHAPTER IV

TEST CONDITIONS AND PROCEDURE

A summary of the wind tunnel test conditions used in the various tests is presented in Table II. Double shielded probes of 0.150, 0.144, 0.056, and 0.020-inch internal diameter probes were tested at Mach numbers 8 and 10 to investigate probe length-to-diameter ratio, L/D , effects on temperature measurements. These probes were fabricated with length-to-diameter ratios as great as 50 and systematically shortened to length-to-diameter ratios of one or zero. Table III, page 17, presents the length-to-diameter ratios tested for various internal diameter probes. The radiation shields were removed from one 0.150-inch internal diameter probe at Mach number 8 and one 0.144-inch internal diameter probe at Mach number 10 to investigate the effect of the number of radiation shields on temperature measurement.

Internal velocity effects on temperature measurements were studied with 0.076-inch internal diameter, single shield, probes at Mach number 8 and with 0.056, 0.076, and 0.144-inch internal diameter probes at Mach number 10. These probes were fabricated with very small vent holes, entrance-to-vent area ratio (A_e/A_v) of 20, and systematically drilled out for successive experiment to an entrance-to-vent area ratio of one. A summary of entrance-to-vent area ratio for various internal diameter probes tested is presented in Table IV, page 18.

TABLE II
TEST CONDITIONS

Probe I.D., in.	Tunnel	M_∞	P_0 , psia	T_0 , °R	$Re \times 10^6$, ft ⁻¹	Remarks
0.150	B	8	100-800	1355	0.5 - 3.8	Standard
	C	10	200-1800	1900	0.3 - 2.2	"
	E	8	400-1600	1170-1480	2.0 - 6.5	"
	B	8	100-800	1355	0.5 - 3.8	
	C	10	200-1800	1900	0.3 - 2.2	
	C	10	200-1800	1900	0.3 - 2.2	
0.144	C	10	225-360	1400-1900	0.5	
	C	10	200-1800	1900	0.3 - 2.2	
0.076	C	10	200-1800	1900	0.3 - 2.2	
	C	10	225-360	1400-1900	0.5	
	E	8	400-1600	1170-1480	2.0 - 6.5	
0.056	C	10	200-1800	1900	0.3 - 2.2	
	C	10	225-360	1400-1900	0.5	
	E	8	400-1600	1170-1480	2.0 - 6.5	
0.020	E	8	400-1600	1170-1480	2.0 - 6.5	

TABLE III
 PROBE LENGTH-TO-DIAMETER RATIO

Probe I.D., in.	L/D
0.150	44.3, 24.3, 7.7, 7.5, 5.0, 4.0, 3.0, 2.0, 1.0, 0.0
0.144	7.5, 5.0, 4.0, 3.0, 2.0, 1.0
0.056	5.0, 3.0, 1.0
0.020	5.0, 3.0, 1.0

TABLE IV
 PROBE ENTRANCE-TO-VENT AREA RATIO

Probe I.D., in.	A_e/A_v
0.150	5.50, 3.00, 2.08
0.144	20.23, 10.23, 5.06, 4.00, 3.08, 1.92, 1.00
0.076	19.99, 10.36, 5.64, 3.61, 2.85, 2.13, 1.00
0.056	19.75, 4.93, 4.30, 3.06, 2.00, 1.00

During all tests a 0.150-inch internal diameter probe, with a length-to-diameter ratio of 5 and an entrance-to-vent area ratio of 5.5, was used as a standard in the wind tunnel test section. All tests were conducted with the standard and probes mounted in the wind tunnel free stream at zero angle of incidence with the flow.

CHAPTER V

ERROR ANALYSIS

A thermocouple can indicate only its own temperature. Any difference between the temperature of the thermocouple junction and the temperature of the medium causes an error in the measured temperature. The total error in the measured temperature can be divided into three categories; velocity error, conduction error, and radiation error (20). In the test run it was necessary to estimate the magnitude of error due to velocity, conduction, and radiation at various run conditions. A method of predicting these errors is by a heat transfer analysis of the thermocouple junction. This is accomplished in the present study by assuming two modes of heat transfer negligible and calculating the error due to the third mode.

I. VELOCITY ERROR

All of the kinetic energy of a flowing gas cannot be recovered as thermal energy at the thermocouple junction. The portion of the kinetic energy recovered is given in Reference 10 as

$$\alpha \equiv \frac{T_j - T_s}{T_o - T_s}, \quad (1)$$

where for a wire parallel to the flow α takes on the essentially constant value of 0.86 in the Mach number range 0.20 to 1.00 (21).

The velocity error is given in Reference 22 as

$$E_v = T_o - T_e = \left[\frac{(1-\alpha) \frac{\gamma-1}{2} M^2}{1 + \frac{\gamma-1}{2} M^2} \right] T_o = \frac{(1-\alpha) u^2}{2g J C_p} \quad (2)$$

The only parameter that may be altered to affect a reduction in velocity error is the velocity. The method of varying velocity was accomplished by varying the vent hole areas. Figure 5 shows the calculated effect of velocity error as a function of Mach number. The velocity error is less than 0.25 per cent if the Mach number is maintained below 0.30 which is equivalent to an entrance-to-vent area ratio of 2. Therefore, as long as the area ratio is greater than 2 the velocity error can be neglected.

II. CONDUCTION ERROR

The conduction error represents the difference in junction temperature and effective temperature; the effective temperature, T_e , is equal to the total gas stream temperature minus the velocity error of the thermocouple junction. The conduction error occurs from conduction of heat through the thermocouple wire to the thermocouple support. By assuming the thermocouple wire is an extended surface or fin of circular cross-section the conduction error is given in Reference 22 as

$$E_c = \frac{T_e - T_{SP}}{\cosh \left(l_w \sqrt{\frac{4h}{k_w d_w}} \right)} \quad (3)$$

In conduction only the effective temperature, T_e , the support

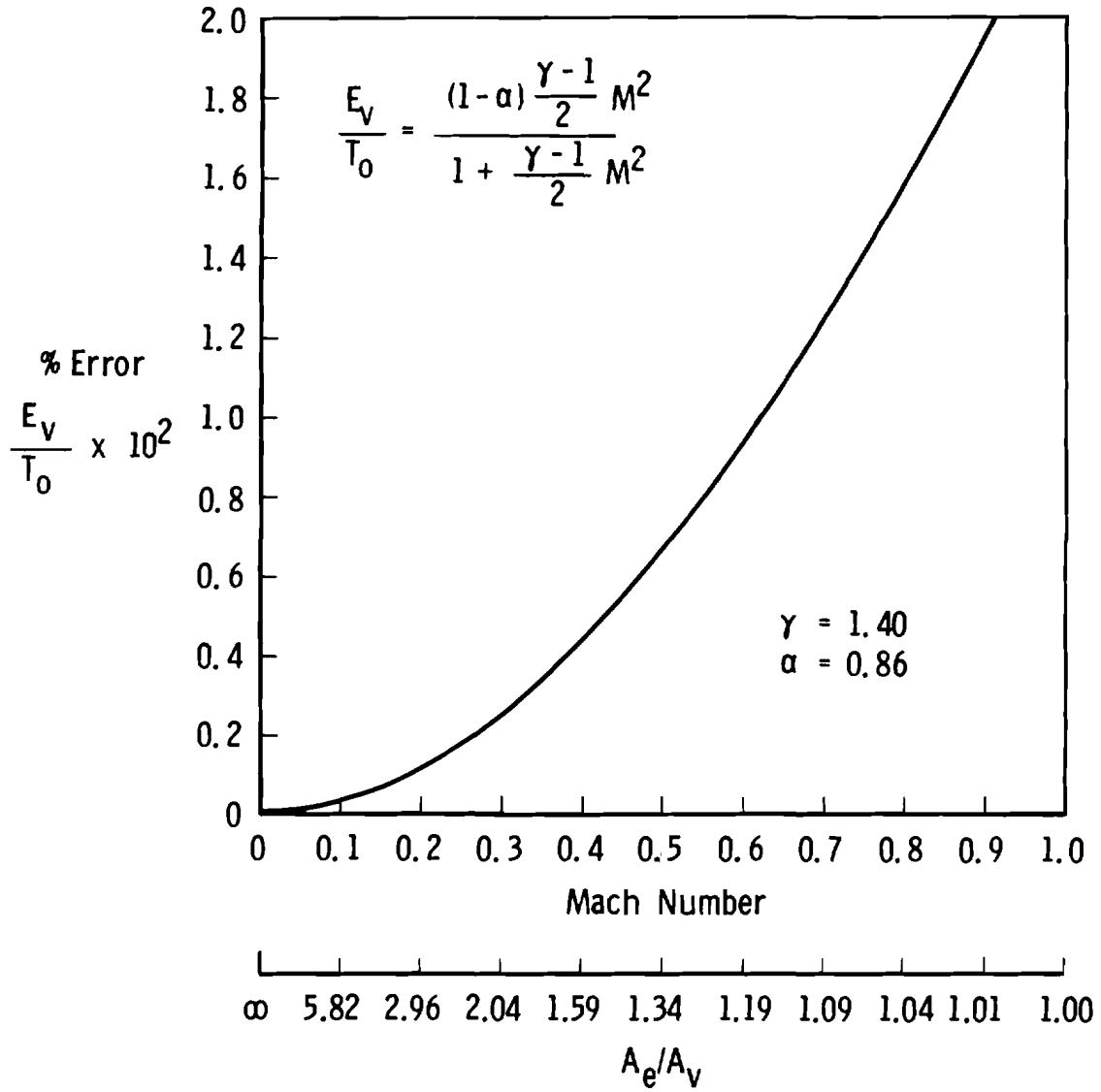


Fig. 5 Per cent Velocity Error as a Function of Mach Number

temperature, T_{sp} , and the convective heat transfer coefficient are predetermined by flow conditions inside the probe. Therefore, the exposed thermocouple wire, l_w , the thermocouple wire diameter, d_w , and the wire thermal conductivity, k_w , may be altered to reduce conduction. The choice of thermocouple wire material is dictated by the temperature levels and the wire diameter is limited by fabrication and durability consideration. Therefore, the only parameters that may be varied is the exposed length of thermocouple wire.

Figure 6 shows the predicted conduction error as a function of internal probe Reynolds number based on the thermocouple wire diameter for various extended wire length-to-wire diameter ratios. The thermocouple wire used was 0.007-inch in diameter. In this investigation the exposed thermocouple wire length-to-diameter was always 50, therefore, conduction loss can be neglected.

III. RADIATION ERROR

Reference 14 gives the radiation error as

$$E_R = \frac{\sigma \epsilon}{h} \sum_{i=1}^n F_{ji} (T_j^4 - T_i^4). \quad (4)$$

As shown in Figure 7, page 25, the thermocouple junction sees two areas, the radiation shield and the tunnel walls. The radiation shield is at approximately the same temperature as the thermocouple junction. Thus, only one configuration factor is needed to calculate the radiation error. The configuration factor can be approximated by the ratio of the solid angle subtended by the open end to the spherical

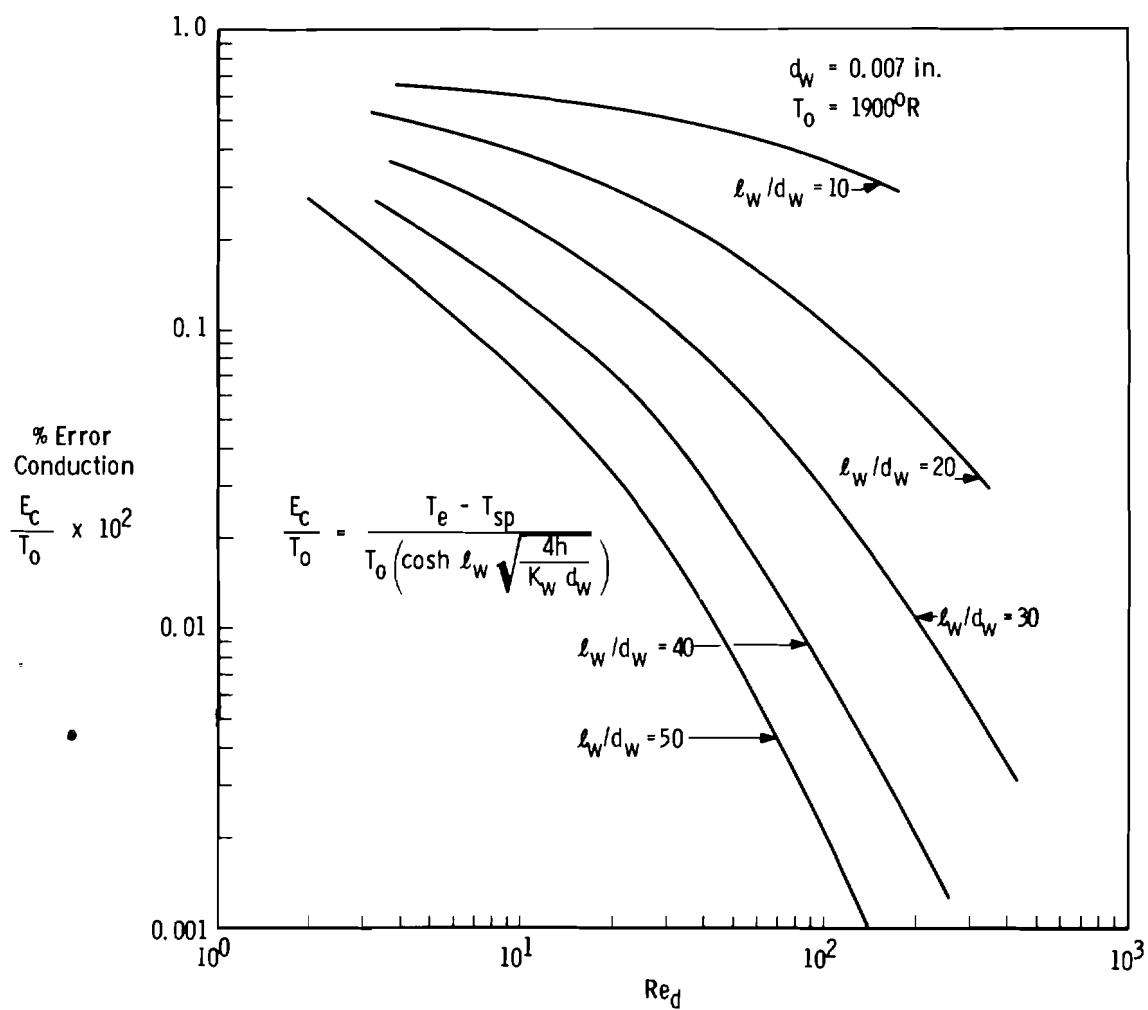
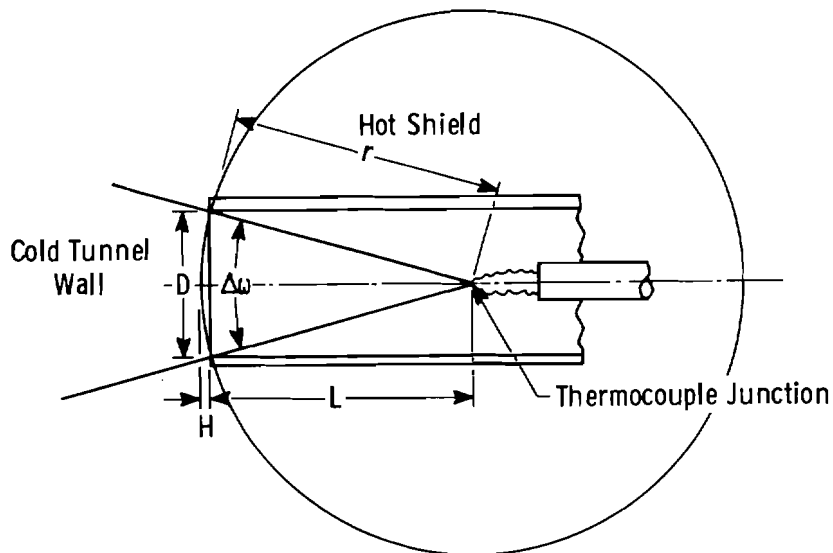


Fig. 6 Conduction Error as a Function of Reynolds Number



$$H = r - L$$

$$r = \left[\left(\frac{D}{2} \right)^2 + L^2 \right]^{1/2}$$

$$F_{ji} = \frac{1}{2} \left[1 - \frac{1}{\left[\left(\frac{D}{2L} \right)^2 + 1 \right]^{1/2}} \right]$$

$$\begin{aligned} \text{Solid Angle } \Delta\omega &= \frac{A_e^*}{r^2} \\ &= \frac{2\pi r H}{r^2} \end{aligned}$$

$$= 2\pi \left[1 - \frac{L}{\left((D/2)^2 + L^2 \right)^{1/2}} \right]$$

*The area of the curved surface of a spherical segment of height, H, radius of sphere, r, (23).

Fig. 7 Configuration Factor

solid angle of 4π steradians,

$$F_{ji} = \frac{\Delta w}{4\pi} = \frac{1}{2} \left[1 - \frac{1}{\left[\left(\frac{D}{2L} \right)^2 + 1 \right]^{1/2}} \right]. \quad (5)$$

The junction temperature, the tunnel wall temperature, and the convective heat transfer coefficient appearing in Equations 4 and 5 are predetermined. The choice of thermocouple wire material dictated by the temperature level fixes the emittance value, ϵ . Thus, only the ratio of L/D may be varied to reduce radiation. It will be shown in Chapter VI that the value of probe length-to-diameter ratio is restricted in order to keep the thermocouple junction located outside of the region of fully developed flow.

Figure 8 shows the magnitude of radiation error as a function of internal probe Reynolds number based on thermocouple wire diameter for various probe length-to-probe internal diameter ratios. Radiation error may be small enough to be neglected in the region where the Reynolds number inside the probe is large or the length-to-diameter ratio is large. In the region of small Reynolds number or where L/D is small, the thermocouple junction temperature may be corrected for radiation losses.

In summarizing the errors it became apparent from Equation 2 that reducing the velocity, u , will decrease the magnitude of the velocity error. It is shown in Figure 5, page 22, that when the vent holes are maintained sonic the per cent of error due to velocity will decrease with decreasing internal Mach number. However, reducing the

7679

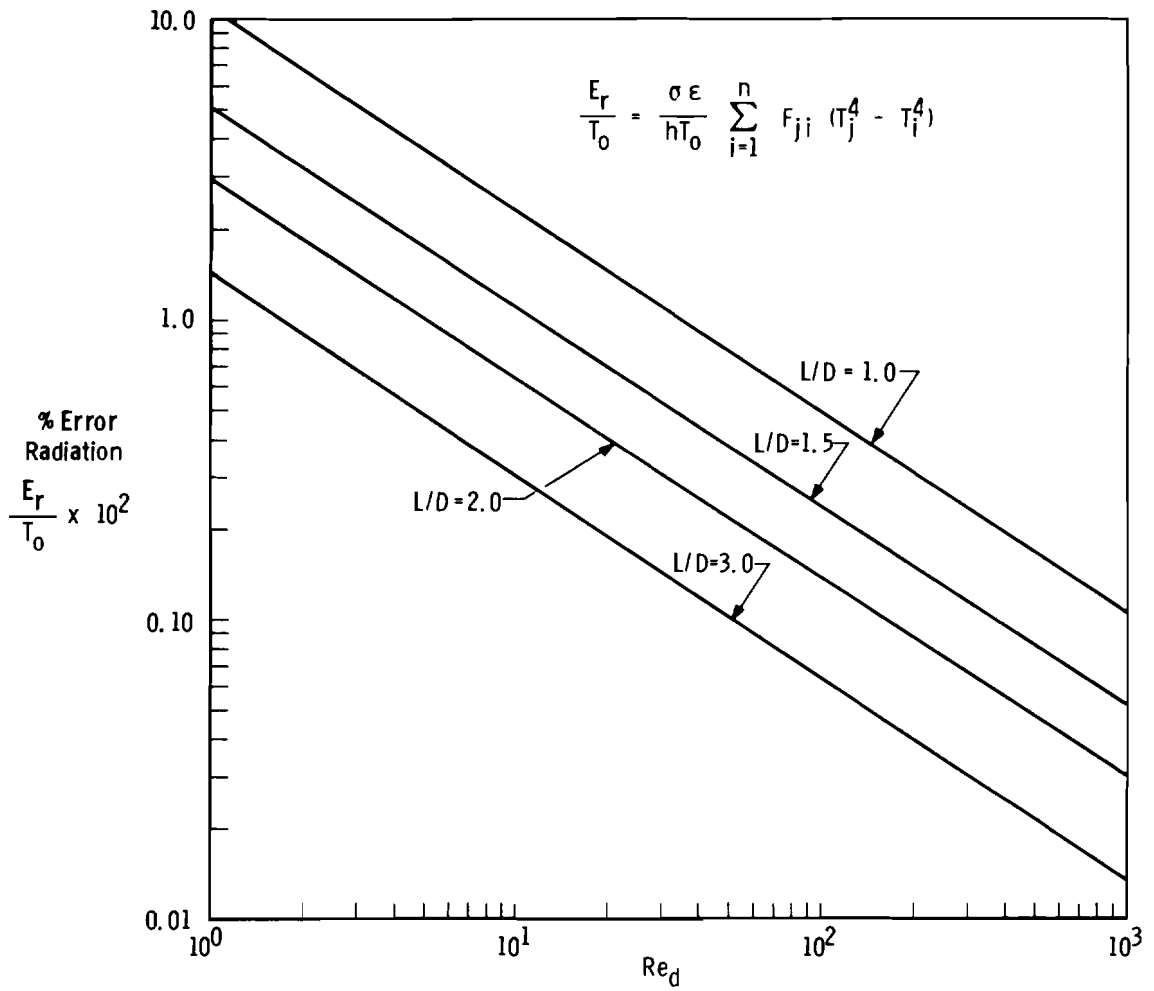


Fig. 8 Per cent Radiation Error as a Function of Reynolds Number

velocity will also reduce the convective heat transfer coefficients which will increase the conduction and radiation errors. To reduce conduction error the thermocouple wire exposed length may be made longer as shown in Figure 6, page 24. Figure 7, page 25, shows to reduce radiation error the thermocouple junction location must be moved further inside the probe. However, there is a limit to how long the exposed thermocouple wire can be and as stated before by moving the thermocouple junction further inside the probe it is possible to get into the region of fully developed flow where there will be viscous losses and conduction losses through the boundary layer. Therefore, there must be a compromise between velocity error, conduction error, and radiation error to get the optimum accuracy. To design a probe, determine the maximum allowable temperature error and then design an environment within which the thermocouple junction can measure the gas temperature within the acceptable accuracy. If it is not possible to design the correct environment then a correction must be made to the temperature measurement to achieve the accuracy required.

CHAPTER VI

THEORETICAL CONSIDERATIONS

It is desirable to have the thermocouple junction near enough to the entrance so that it is not within the region of fully developed flow of the inner shield. The entrance length or region of under-developed flow in the probe was computed for each geometry and tunnel test condition and used in the data correlation. The entrance length, L_e , was estimated from the theory of Boussinesq as given in Reference 24,

$$L_e/D = 0.065 \frac{\dot{\omega}D}{\mu_e A_e} \quad (6)$$

Using the definition of $\dot{\omega}$

$$\dot{\omega} = \rho_e u_e A_e \quad (7)$$

Equation 6 can be written

$$L_e/D = 0.065 \frac{\rho_e u_e D}{\mu_e} = 0.065 Re_{e,D} \quad (8)$$

where the Reynolds number, $Re_{e,D}$, is based upon conditions at the probe entrance.

$\rho_e u_e$ was computed by applying the continuity equation at the probe entrance and exit

$$\rho_e u_e = \rho_v u_v \frac{A_v}{A_e} \quad (9)$$

assuming a low velocity, perfect gas inside the probe and sonic flow through the probe vent holes. The velocity at the vent holes is given in Reference 25 as

$$u_v = a_v = \left(\frac{a_v}{a_e} \right) a_e = \left(1 + \frac{\gamma-1}{2} \right)^{-0.5} (\gamma R T_e)^{0.5} . \quad (10)$$

ρ_v is given in Reference 26 as

$$\rho_v = 0.634 \rho_e = 0.634 \frac{P_e}{R T_e} . \quad (11)$$

Substituting Equations 10, 11, and γ for an ideal gas (1.4) into Equation 9 and simplifying gives

$$\rho_e u_e = 0.684 \frac{P_e}{R T_e} (R T_e)^{0.5} A_e / A_e . \quad (12)$$

The entrance area, A_e , is

$$A_e = \frac{\pi D^2}{4} . \quad (13)$$

Substituting Equations 12, 13, and R (1716.3 ft²/sec²-°R) into Equation 8 and simplifying gives

$$L_e = 1.37 \times 10^{-3} p_e A_v / \mu_e T_e^{0.5} . \quad (14)$$

The entrance length, L_e , was computed from Equation 14 using the tunnel free-stream pitot pressure for p_e , tunnel stilling chamber temperature, T_0 , for T_e , and Sutherland's viscosity equation as given in Reference 25

$$\mu_e = 2.27 \times 10^{-8} \frac{(T_0)^{1.5}}{198.7 + T_0} . \quad (15)$$

CHAPTER VII

RESULTS AND DISCUSSION

The first requirement of this study was to obtain experimental temperature data for various length-to-diameter ratio probes in order to investigate the effect of thermocouple junction location on temperature measurements. This was accomplished by starting in Tunnel B at Mach number 8 with a fairly large probe, 0.150-inch internal diameter, with a length-to-diameter ratio of 44.3 then systematically cutting it off to a length-to-diameter ratio of one. Results of this test are presented in Figure 9a which show that decreasing length-to-diameter ratios increases the temperature ratios. It is shown that for a length-to-diameter ratio of approximately five, the thermocouple junction temperature is within 2 per cent of the stagnation temperature at all pressure levels. Figure 9b shows the length-to-diameter ratio effects on a 0.150-inch internal diameter probe at Mach number 10. The temperature ratio increased with decreasing length-to-diameter ratio until at a length-to-diameter ratio of one, the junction temperature is within 2 per cent of the stagnation temperature at all pressure levels. Ideally, the ratio of junction-to-stagnation temperature ratio should be one, although based on the thermocouple wire manufacturer's literature, a knowledge of VKF temperature recording system, and from the error analysis there may be a total error of ± 2 per cent.

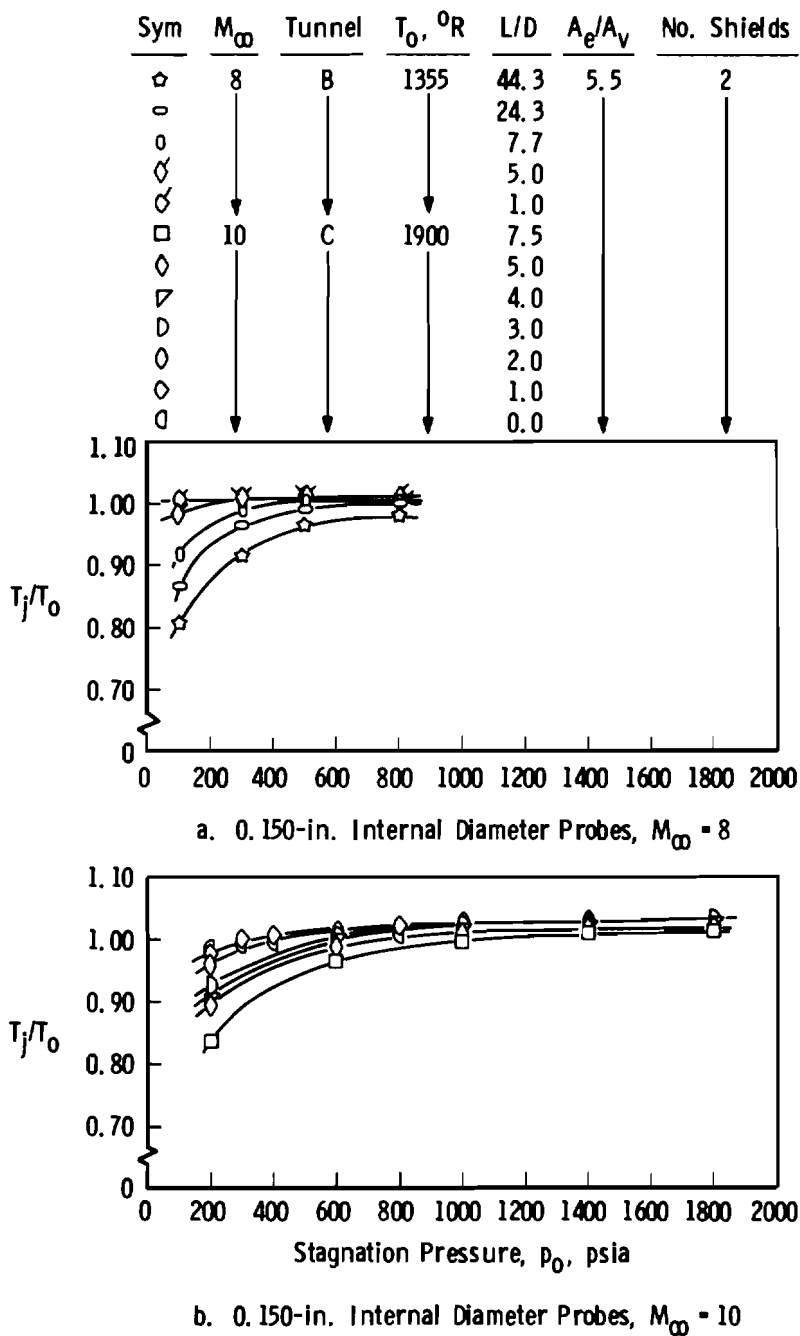


Fig. 9 Effect of Stagnation Pressure on Measured Temperature Ratio at Various Length-to-Diameter Ratios for 0.150-inch Internal Diameter Probes

The Mach number 10 data, Figure 9b, shows that the temperature ratio at high stagnation pressure gets as high as 1.04. From the calibrations of the stagnation temperature probes and the probes being investigated it was shown that the probes were within the manufacturer's specification of ± 1 per cent. Hence the gas at the thermocouple junction is at a higher temperature than the stagnation temperature. At the highest stagnation pressure levels there is a real gas effect which accounts for approximately 1 per cent increase in temperature at the thermocouple junction. The remaining increase in temperature may be due to uncertainties involved in the measurement of a true tunnel stagnation temperature, losses to the nozzle walls, and possible non-uniform temperature distribution in the free-stream flow.

After the initial investigation at Mach number 10 it was determined that a 0.144-inch internal diameter probe which can be constructed of standard thin wall tubing was easier to construct and also as easy to make geometry changes. After the initial investigation all probes were constructed of standard tubing.

Data for a 0.144-inch internal diameter probe are presented in Figure 10a to show the effects of thermocouple junction location on measured temperature ratios at Mach number 10. The temperature ratio increased with decreasing length-to-diameter ratio, though the temperature ratio is never greater than 95 per cent for the low stagnation pressure levels. Probes of 0.056 and 0.020-inch internal

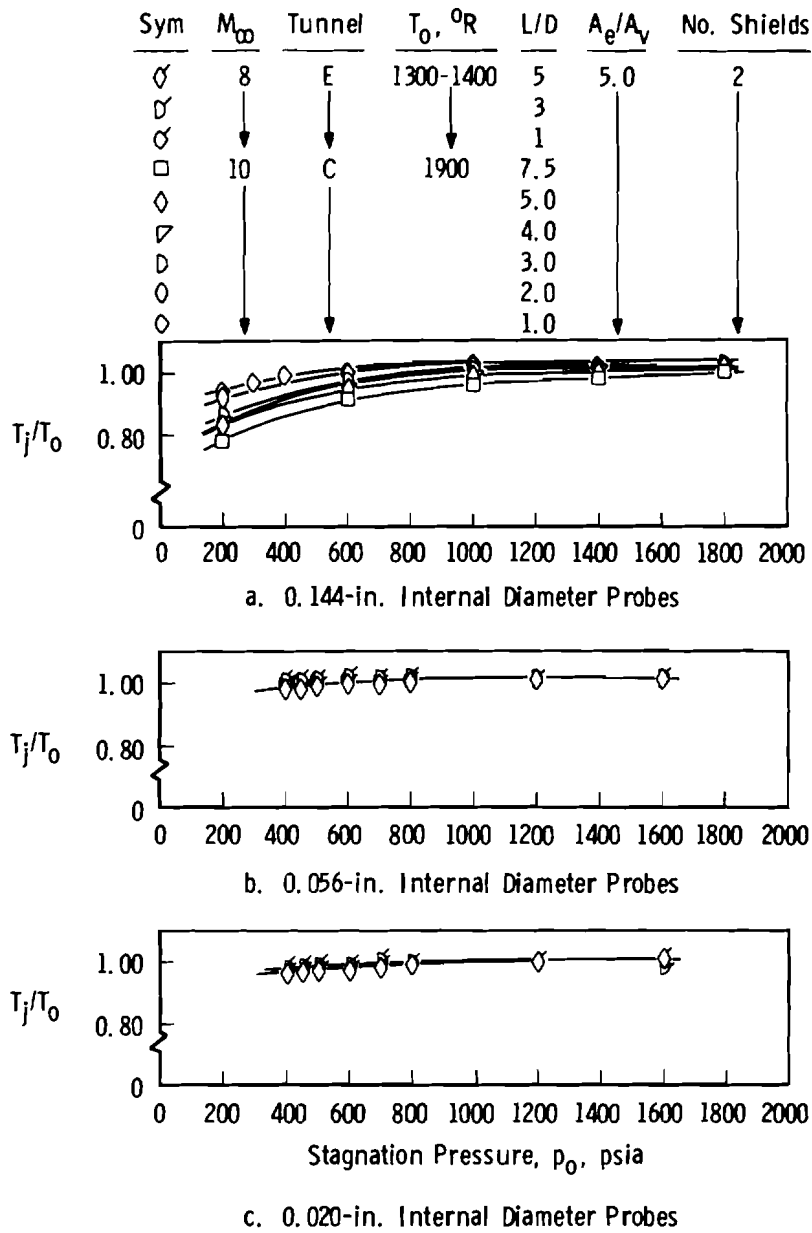


Fig. 10 Effect of Stagnation Pressure on Measured Temperature Ratio at Various Length-to-Diameter Ratios

diameter were tested at Mach number 8 to determine the effects of length-to-diameter ratio on temperature measurements. These data are presented in Figures 10b and 10c. For the 0.056-inch internal diameter probes the temperature ratio reached one for a length-to-diameter ratio of three. The data from the 0.020-inch internal diameter probes, Figure 10c, appear nonsystematic with varying length-to-diameter ratio. This may have been caused by the inability to cut the small tube off smoothly and also the inability to clean all burrs out of the entrance of the probe after cutting the probes off.

The effect of thermocouple junction location on measured temperature ratios at four pressure levels is presented in Figure 11. The temperature ratios, Figure 11a, for the 0.144-inch internal diameter probe never reached one for the 200 psia stagnation pressure level, however, for the other stagnation pressure levels the junction temperature reached 100 per cent of the stagnation temperature at a length-to-diameter ratio of two. The temperature ratio for a 0.150-inch internal diameter, Figure 11b, shows that the junction temperature reaches 98 per cent of the stagnation temperature at a length-to-diameter ratio of one for a stagnation pressure of 200 psia. For all other pressure levels the temperature ratio reaches one for a length-to-diameter ratio of three. For the investigation of thermocouple junction location all probes tested had an entrance-to-vent area ratio of 5.0 except the 0.150-inch internal diameter probes which had an area ratio of 5.5.

It is apparent from Figure 11 that as the length-to-diameter

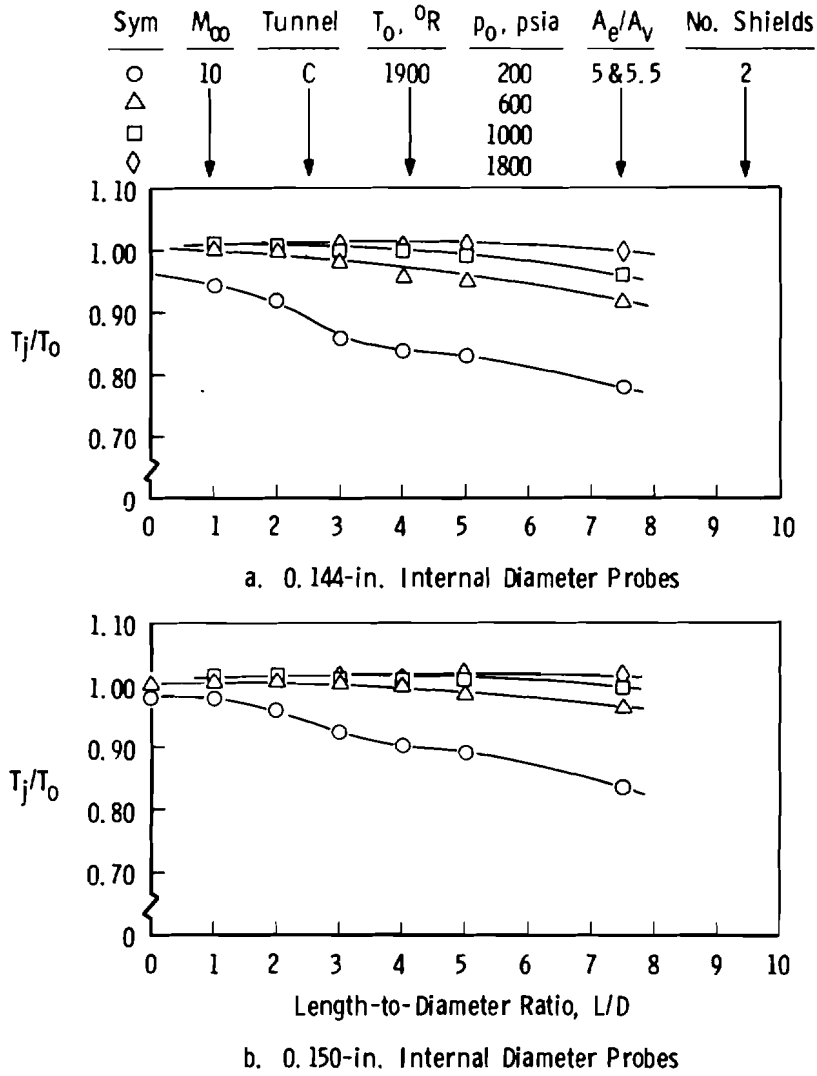


Fig. 11 Effect of Length-to-Diameter Ratio on Measured Temperature Ratio

ratio increases the temperature ratio decreases. This temperature decrease must be accounted for by some error other than the losses of velocity, conduction, and radiation errors. All probes tested had the same area ratios or velocity error, same exposed thermocouple wire length or conduction error, and as shown in Figure 8, page 27, as length-to-diameter ratio increased the radiation error decreased. The error calculated for a 0.144-inch internal diameter probe with an area ratio of 5.0 and an exposed thermocouple wire length-to-diameter ratio of 50 is presented in Table V for the four pressure levels presented in Figure 11a. The data presented in this chapter have not been corrected for errors.

It has been observed that for a length-to-diameter ratio of two and a pressure level of 200 psia a portion of the exposed wire is in the region of fully developed flow. This may account for some error. For a length-to-diameter ratio greater than three at a stagnation pressure of 200 psia the thermocouple junction is in a region of fully developed flow. Hence additional error may be accounted for due to viscous effects and conduction through the boundary layer to the radiation shields.

The second requirement of this study was to obtain experimental data for various internal diameter probes in order to determine the optimum entrance-to-vent area ratio. This was accomplished by starting with a 0.150-inch internal diameter probe at Mach number 10 and varying the entrance-to-vent area ratio from 5.5 to 2.08. As shown in Figure 12a, page 39, for an area ratio of three or less and length-to-

TABLE V
 ERROR FOR A 0.144-INCH INTERNAL DIAMETER PROBE

P_0 , psia	L/D	E_v per cent	E_c per cent	E_r per cent	Total Error, per cent
200	1	0.038	0.150	4.219	4.407
	2	0.038	0.150	1.198	1.386
	3	0.038	0.150	0.551	0.739
600	1	0.038	0.060	2.100	2.198
	2	0.038	0.060	0.585	0.683
	3	0.038	0.060	0.278	0.276
1000	1	0.038	0.035	1.517	1.590
	2	0.038	0.035	0.431	0.504
	3	0.038	0.035	0.198	0.271
1800	1	0.038	0.015	0.010	1.063
	2	0.038	0.015	0.287	0.340
	3	0.038	0.015	0.132	0.185

As

T ...

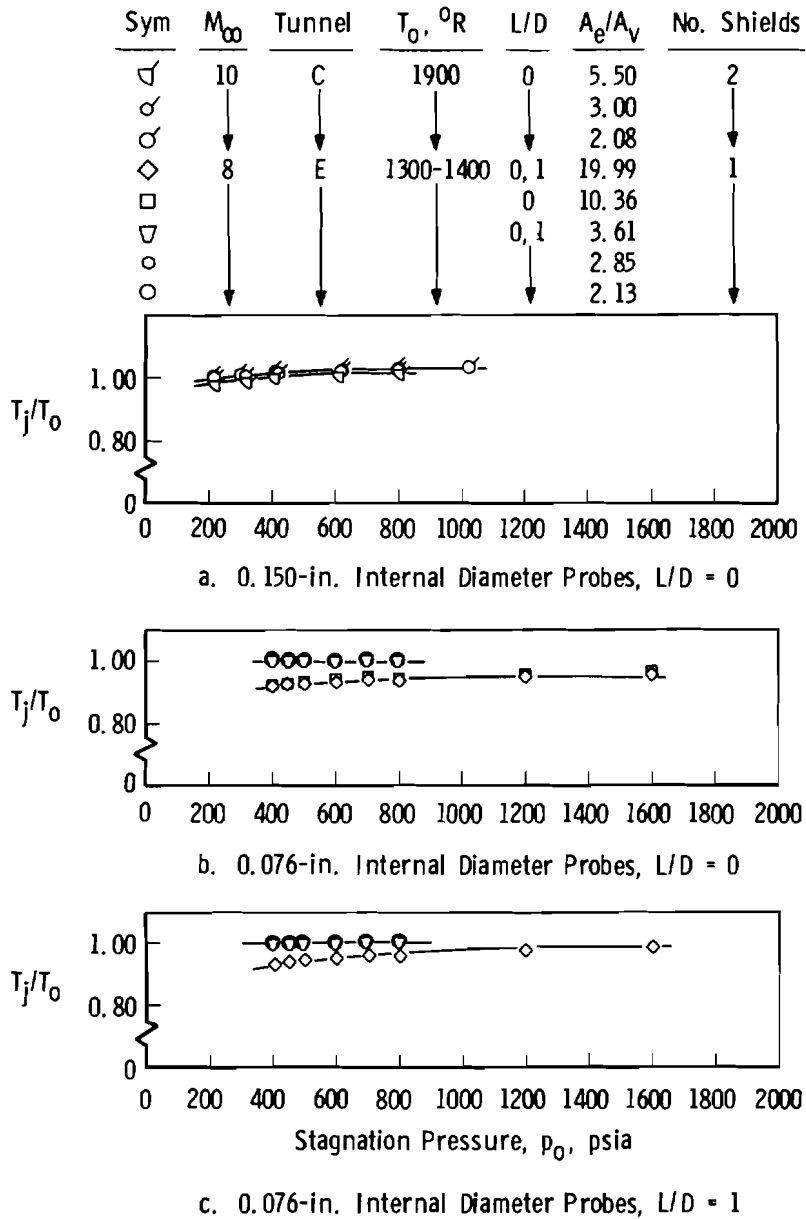


Fig. 12 Effect of Stagnation Pressure on Measured Temperature Ratio at Various Entrance-to-Vent Area Ratios

diameter ratio of zero the temperature ratio of the junction temperature-to-stagnation temperature was equal to one for all pressure levels tested. Mach number 8 data for a 0.076-inch internal diameter probe are presented in Figure 12b and 12c which show that for area ratio of 3.6 or less and length-to-diameter ratios of zero or one the temperature ratio is equal to one.

Mach number 10 data are presented in Figures 13, 14, and 15 to show the effects of entrance-to-vent area ratio or internal velocity on the temperature measurements for various internal diameter probes. The trend for all size probes is that the ratio of thermocouple junction-to-stagnation temperature increased with decreasing entrance-to-vent area ratio. For the 0.144-inch internal diameter probe the temperature ratio reached one for all stagnation pressure levels at an area ratio of three and a length-to-diameter ratio of two, Figure 13. The data for the smaller probes are presented in Figures 14 and 15, pages 42 and 43, which show that the temperature ratio did not reach one for the lower stagnation pressure levels. This may have been caused by the inability to drill out all vent holes to the exact size and also the inability to clean all burrs out of the vent holes. The junction-to-stagnation temperature ratio got as large as 1.04 at the higher stagnation pressure levels; this may be due to real gas effects and tunnel inaccuracies as stated before. Figure 16, page 44, shows that for length-to-diameter ratios of 1, 2, and 3 the junction-to-stagnation temperature equals one for all entrance-to-vent area ratios less than three for a 0.144-inch internal diameter probe. For a 0.076-

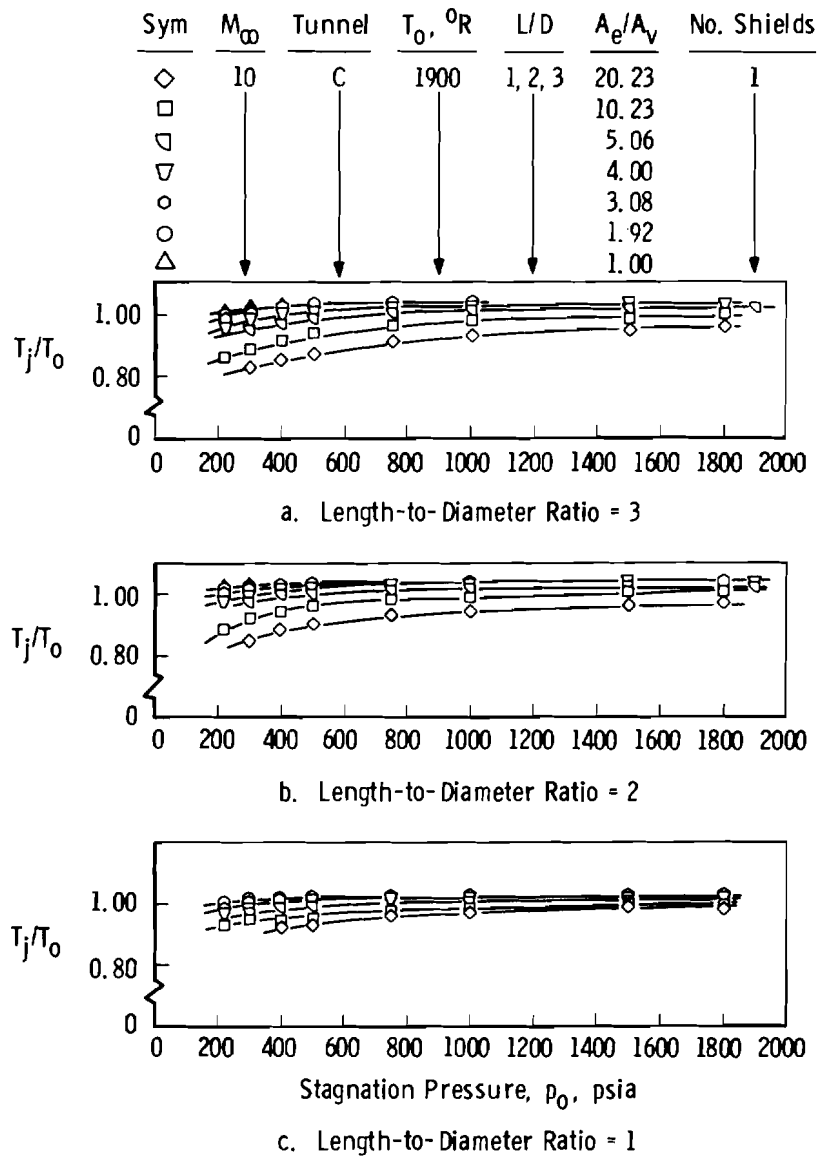


Fig. 13 Effect of Stagnation Pressure on Measured Temperature Ratio at Various Entrance-to-Vent Area Ratios for 0.144-inch Internal Diameter Probes

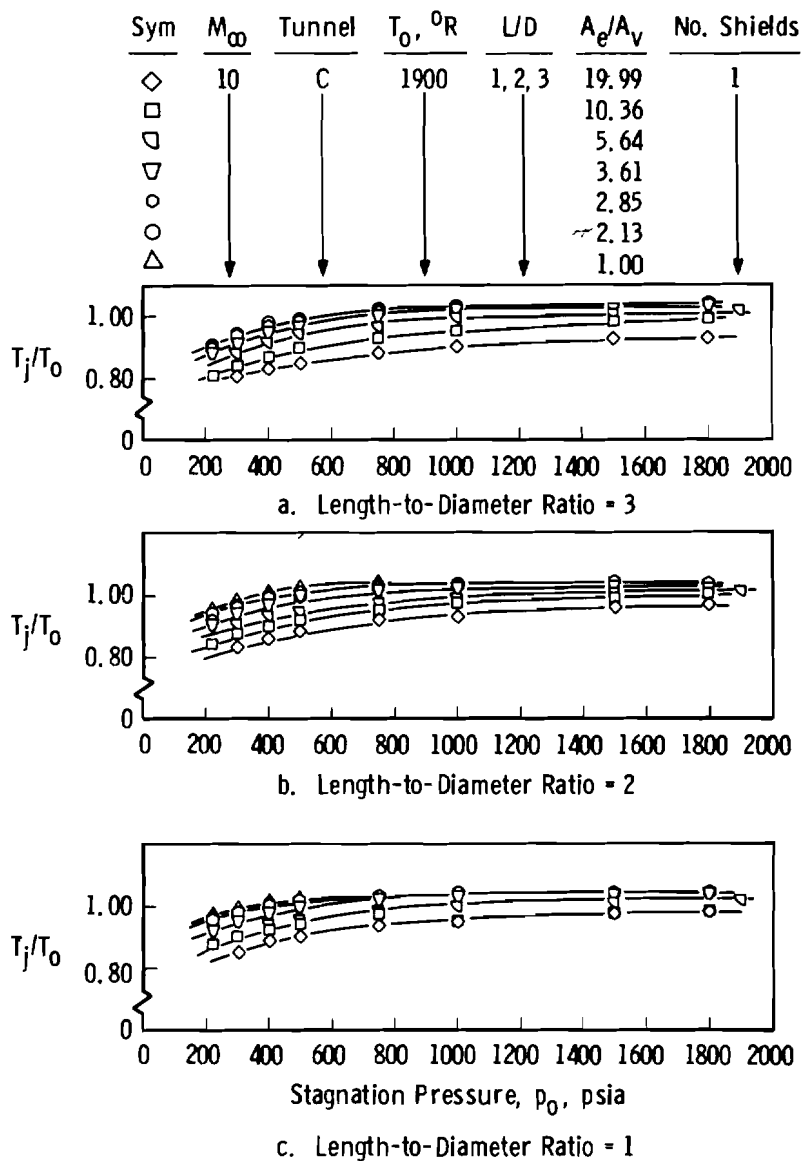


Fig. 14 Effect of Stagnation Pressure on Measured Temperature Ratio at Various Entrance-to-Vent Area Ratios for 0.076-inch Internal Diameter Probes

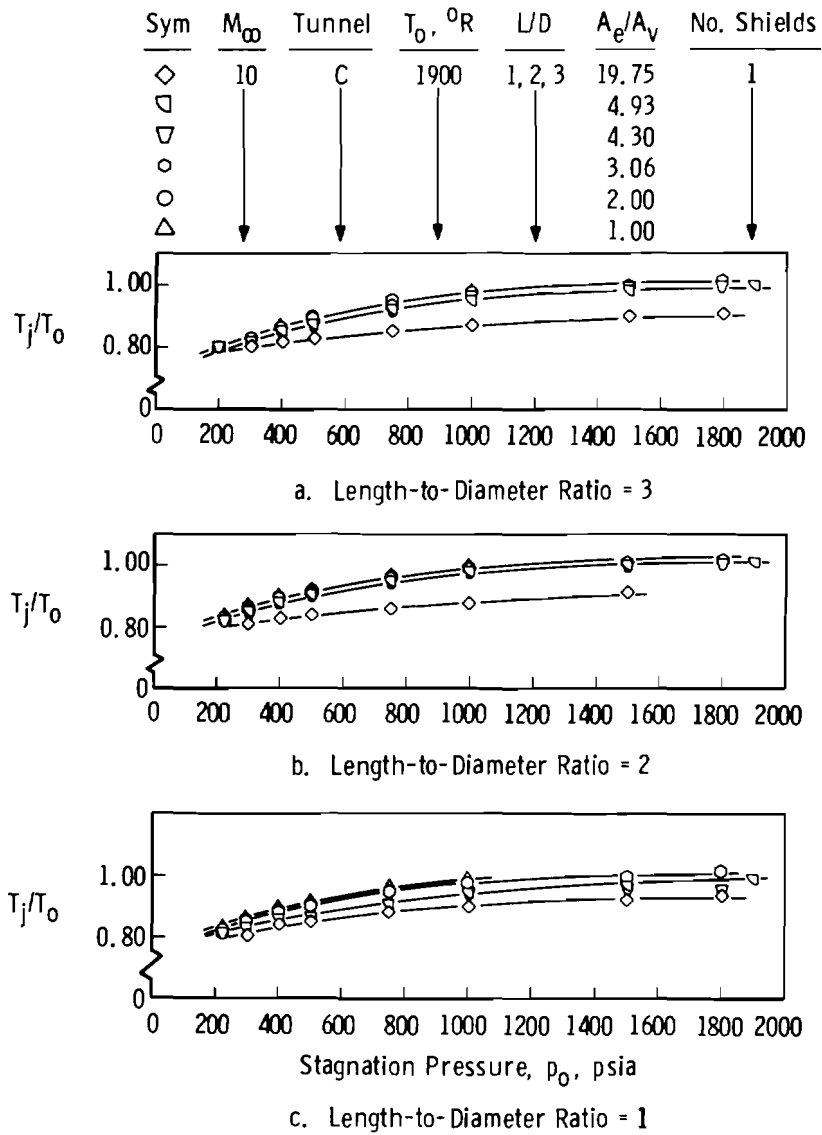


Fig. 15 Effect of Stagnation Pressure on Measured Temperature Ratio at Various Entrance-to-Vent Area Ratios for 0.056-inch Internal Diameter Probes

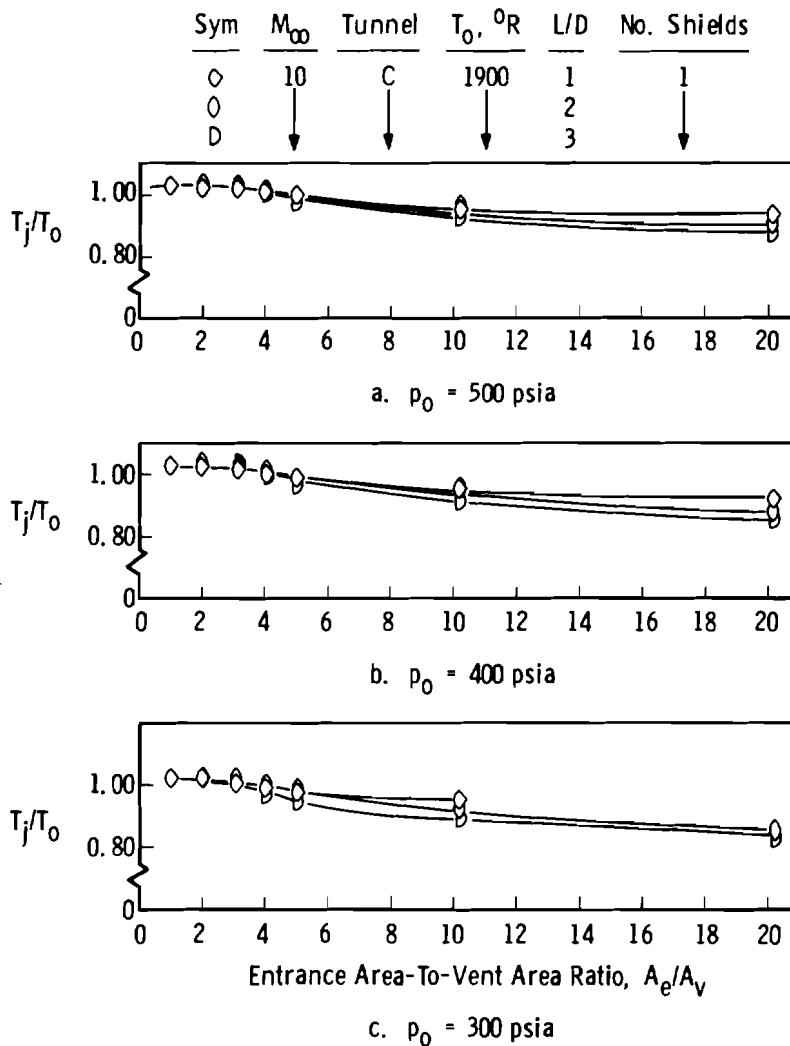


Fig. 16 Effect of Entrance Area-to-Vent Area Ratio on Measured Temperature Ratio at Various Length-to-Diameter Ratios for 0.144-inch Internal Diameter Probes

inch internal diameter probe, Figure 17 shows that for only a length-to-diameter ratio of 1 or 2, will the temperature ratio reach 98 per cent for an area ratio of less than three. From Figures 16 and 17 it is shown that the optimum entrance-to-vent area ratios are less than three and the optimum length-to-diameter ratio is two.

The effects of removing the probe radiation shields at Mach numbers 8 and 10 are presented in Figure 18, page 47. The maximum effect of removing the outer shield was to decrease the temperature ratio by one per cent at Mach number 10 as shown in Figure 18a. Removing both shields decreased the temperature ratio about 10 per cent at Mach number 8 and 15 per cent at Mach number 10.

The effects of stagnation pressure and temperature on junction-to-stagnation temperature ratio at Mach number 10 and constant free-stream Reynolds number are presented in Figure 19, page 48. For 0.144- and 0.076-inch internal diameter probes there was no effect on the temperature at the thermocouple junction as shown in Figures 19a and 19b, respectively. By increasing the stagnation pressure and temperature, the temperature ratio decreased for a 0.056-inch internal diameter probe as shown in Figure 19c. The temperature ratio decreased a maximum of 2 per cent over the range tested.

The performance of the proposed correlation parameter, the entrance length-to-probe length ratio, L_e/L , is shown in Figures 20 through 22, pages 49 through 51. At values of $L_e/L > 1$ the thermocouple junction is in the entrance core region of flow and the measured temperature should read the stilling chamber temperature. At

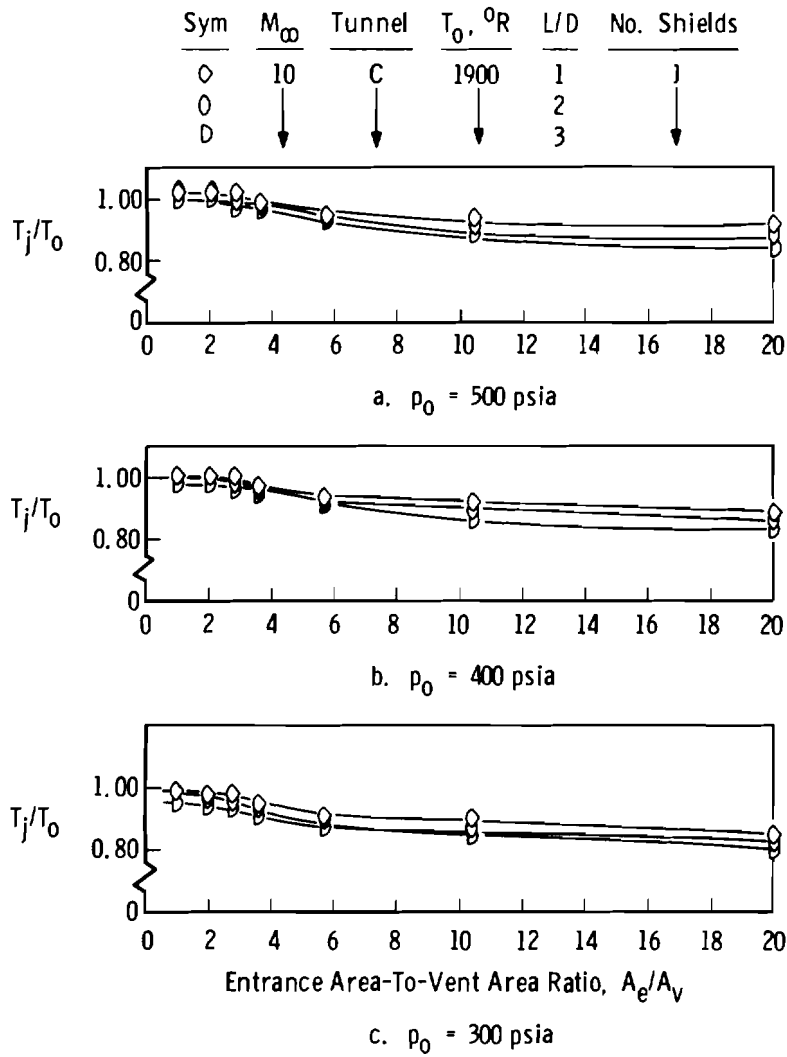


Fig. 17 Effect of Entrance Area-to-Vent Area Ratio on Measured Temperature Ratio at Various Length-to-Diameter Ratios for 0.076-inch Internal Diameter Probes

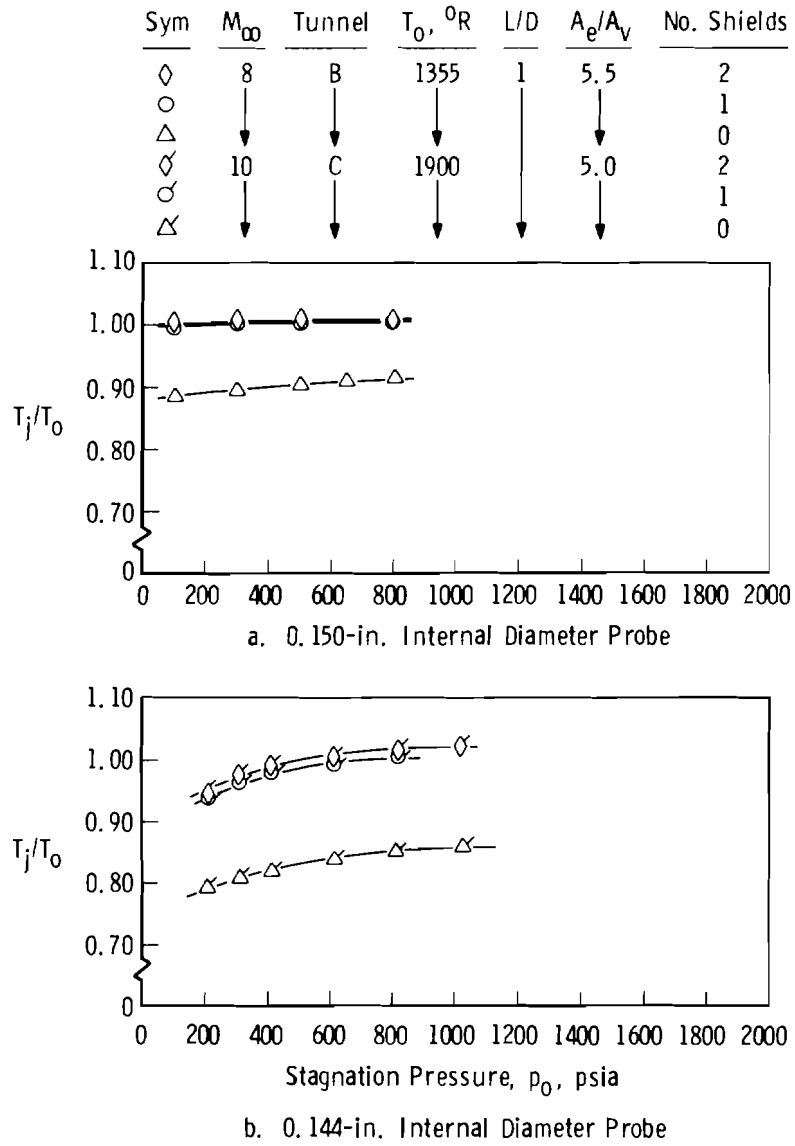


Fig. 18 Effect of Radiation Shields on Measured Temperature Ratios

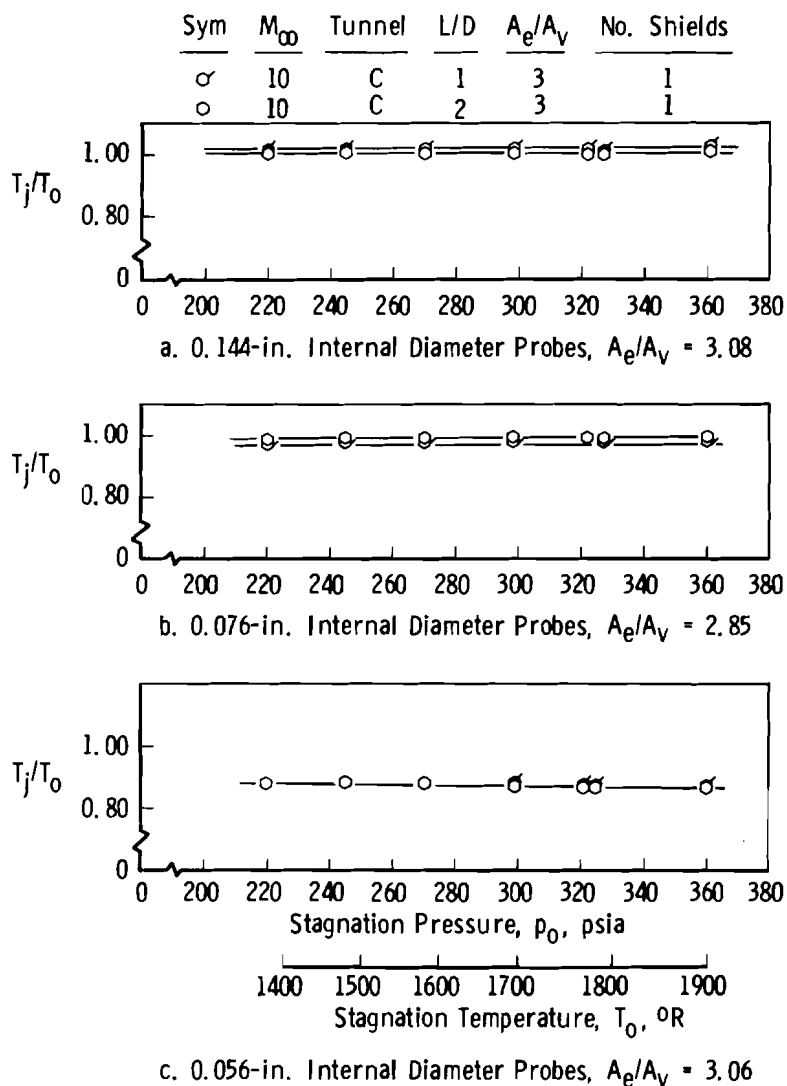


Fig. 19 Effect of Stagnation Pressure and Temperature on Measured Temperature Ratios at a Constant Free-Stream Reynolds Number of $0.5 \times 10^6 \text{ ft}^{-1}$

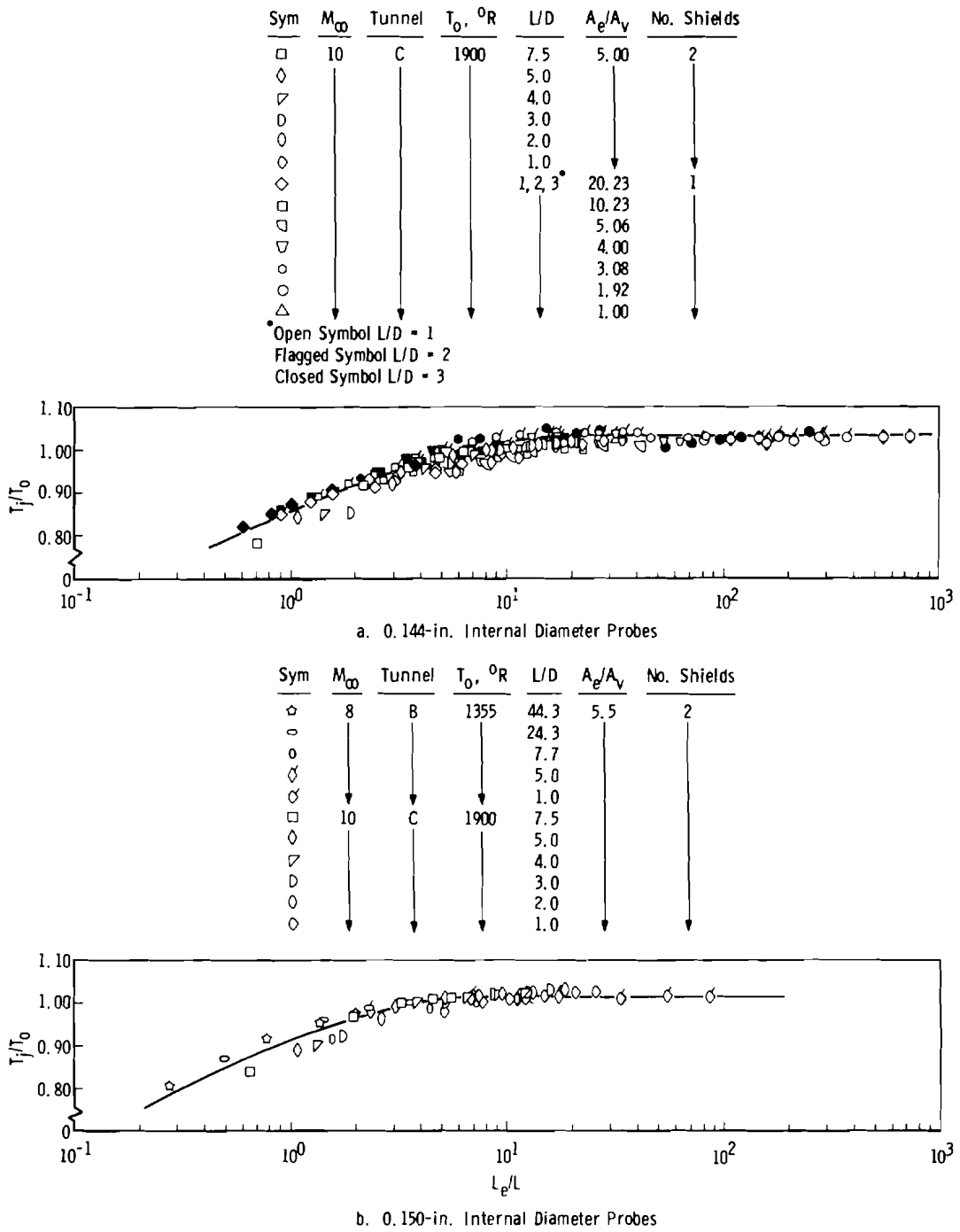
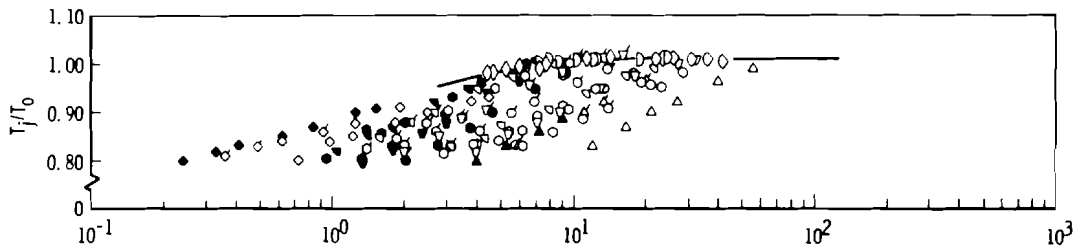


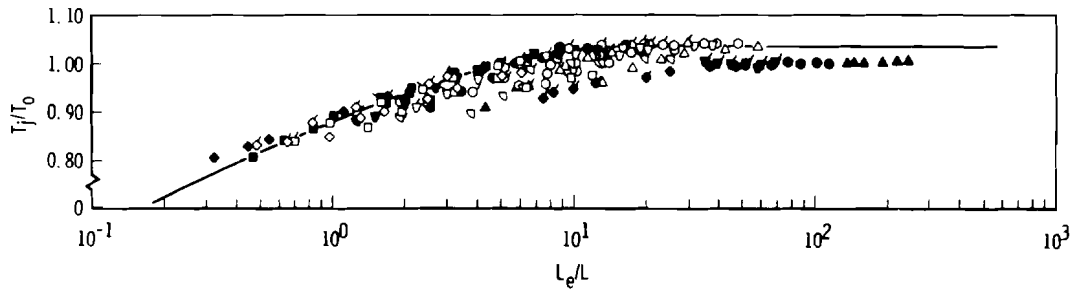
Fig. 20 Temperature Ratio as a Function of L_e/L for Probes of 0.144- and 0.150-inch Internal Diameter

Sym	M_∞	Tunnel	$T_0, ^\circ R$	L/D	A_e/A_v	No. Shields
◇	8 & 10	C & E	1900 & 1300-1400	1, 2, 3	19.99	1, 2
□	10	C	1900		10.36	1
▽	10	C	1900		5.64	1
◊	8 & 10	C & E	1900 & 1300-1400		3.61	1, 2
○					2.85	
◌					2.13	
△					1.00	

Open Symbols L/D = 1, $M_\infty = 10$
 Flagged Symbol L/D = 2, $M_\infty = 10$
 Closed Symbol L/D = 3, $M_\infty = 10$
 Closed Flagged Symbol L/D = 1, $M_\infty = 8$



a. 0.056-in. Internal Diameter Probes



b. 0.076-in. Internal Diameter Probes

Fig. 21 Temperature Ratio as a Function of L_e/L for Probes of 0.056- and 0.076-inch Internal Diameter

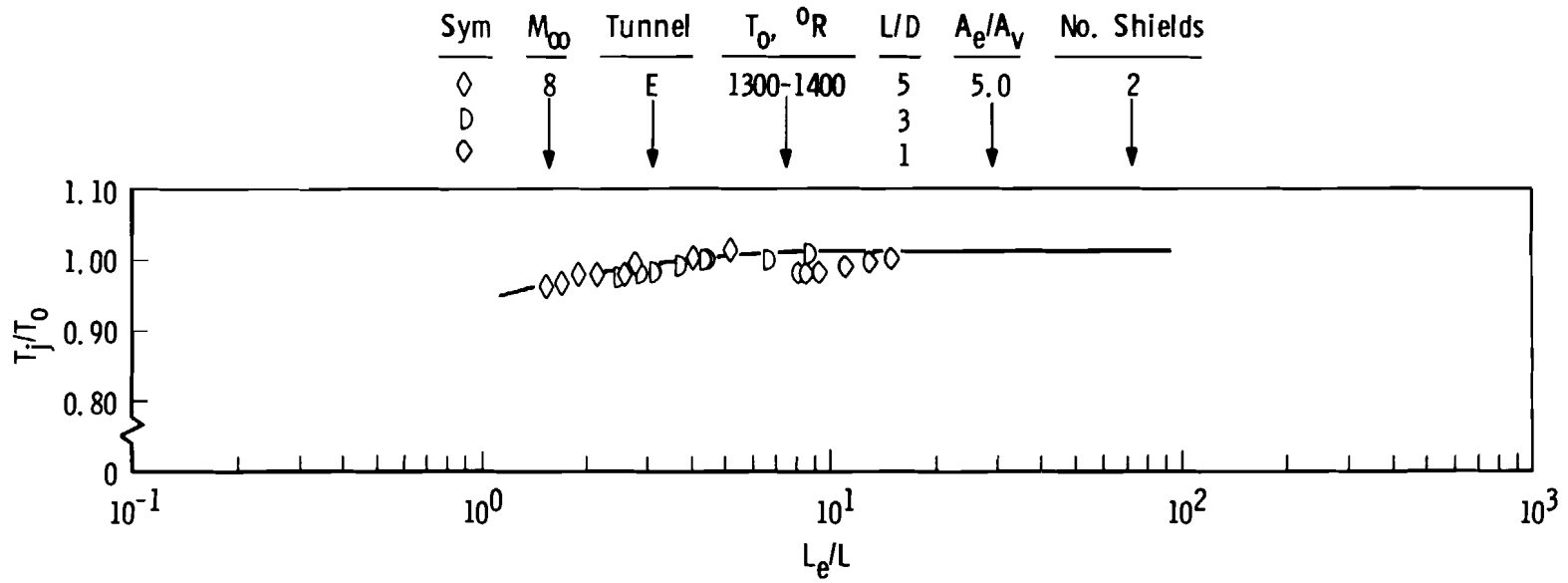


Fig. 22 Temperature Ratio as a Function of L_e/L for 0.020-inch Internal Diameter Probes

values of $L_e/L < 1$ the junction is in the region of fully developed boundary layer and would be expected to experience viscous losses and conduction losses through the boundary layer. It is apparent from Figures 20, 21, and 22 that values of $L_e/L \approx 10$ are required to achieve temperature ratio, T_j/T_o , of one. Little significance is attached to the specific level of L_e/L since the physical size of the thermocouple and the choice of entrance flow length theories would be expected to play important roles.

Figures 20, 21b, and 22 show that entrance length-to-probe length effectively correlates data for probes of the same diameter for various stagnation temperatures, free-stream Mach numbers, length-to-diameter ratios, and entrance-to-vent area ratios. It is apparent in Figure 21a, page 50, that data for the 0.056-inch internal diameter probes do not correlate. This may be accounted for by the inaccuracies in drilling out the small probes as stated before. Hence, the vent area used in calculating the entrance length may be in error. The curve faired in Figure 21a is faired through the data for various length-to-diameter ratio.

A summary of the correlation data presented in Figures 20, 21, and 22 is presented in Figure 23. The failure of the correlation parameter to account for various internal diameters is obvious in Figure 23. The measured temperature ratio is not systematic with internal diameter at a constant entrance length-to-probe length ratio. However, it has been observed that the distance between the inner and outer shield was not scaled precisely for the various diameter probes.

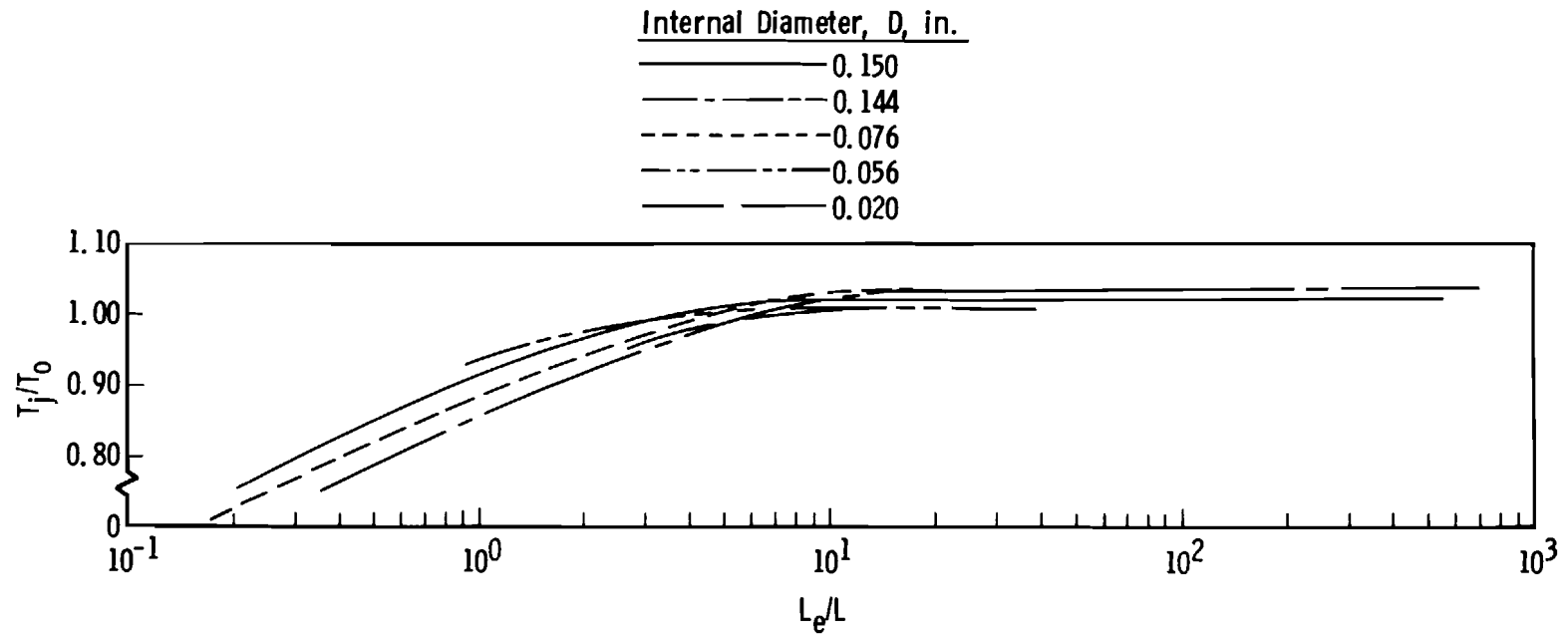


Fig. 23 Summary of Correlation Data

It is also noted that the distance from the thermocouple junction to the inner shield was not the same for all internal diameter probes tested. Since the distance is different between the two shields for various diameter probes, the region between the shields will become fully developed at various probe lengths. This creates a lower temperature on the inner shield due to viscous effects and conduction to the outer shield. The entrance length, L_e , is for fully developed flow in the tube, however since the thermocouple junction has a physical dimension it is in the boundary layer before the tube is fully developed. If the distance from the thermocouple junction to the inner shield is different for one internal diameter probe than for another the junction will be in the boundary layer at different entrance length-to-probe length ratios. This creates a greater viscous loss for one probe than for another. Also because the inner shields may be at a different temperature for one probe than for another there will be greater conduction loss through the boundary layer. This may account for the reason that various diameter probes will not correlate for this correlation parameter.

Given a probe internal diameter required for a particular investigation one can use the correlation parameter to calculate the Reynolds number range in which the probe will give the required accuracy. An example of how this Reynolds number range can be calculated is presented. Assuming an internal probe diameter, D , of 0.020-inch and an accepted accuracy of ± 1 per cent, the optimum length-to-diameter ratio is two, therefore, the length, L , equals 0.040 inch.

From Figure 22, page 51, for a temperature ratio of one $L_e/L \cong 10$, therefore, $L_e \cong 0.40$. Using Equation 8 and by knowing D and L_e one can calculate $Re_{e,D} \cong 300$.

CHAPTER VIII

CONCLUSIONS

Experimental data were obtained for Mach numbers 8 and 10 over a free-stream Reynolds number range of 0.3 to $6.5 \times 10^{-6} \text{ ft}^{-1}$ to determine the effects of thermocouple junction location and internal velocity, and radiation shields on measured junction-to-stagnation temperature ratio. By comparison of the experimental data over the range of this investigation the following conclusions can be made:

1. During the investigation of thermocouple junction location all measured temperatures increased with decreasing length-to-diameter ratios.
2. During the investigation of internal velocity all measured temperatures increased with decreasing entrance-to-vent area ratios.
3. The optimum length-to-diameter ratio is two and the optimum entrance-to-vent area ratio is two over the range investigated.
4. For the correlation parameter used, entrance length-to-probe length ratio, L_e/L , the measured temperature ratio equals one for a $L_e/L > 10$.
5. Additional work should be done on a correlation parameter to try and get a correlation for probes of various internal diameter.

BIBLIOGRAPHY

BIBLIOGRAPHY

1. Hottel, J. C. and A. Kalitinsky. "Temperature Measurements in High-Velocity Air Stream," Journal of Applied Mechanics, 12: A25-A32, March, 1945.
2. Franz, A. "Pressure and Temperature Measurement in Supercharger Investigation," National Advisory Committee for Aeronautics Technical Memorandum 953, Washington, D. C., September, 1940.
3. Wimmer, W. "Stagnation Temperature Recording," National Advisory Committee for Aeronautics Technical Memorandum 967, Washington, D. C., January, 1941.
4. Eckert, E. "Temperature Recording in High-Speed Gas," National Advisory Committee for Aeronautics Technical Memorandum 983, Washington, D. C., 1941.
5. Lindsey, W. F. "Calibration of Three Temperature Probes and a Pressure Probe at High Speeds," National Advisory Committee for Aeronautics War Report, Washington, D. C., April, 1942.
6. Malmquist, Lars. "Temperature Measurements in High-Velocity Gas Stream," Transactions of the Royal Institute of Technology Report 15, Stockholm, Sweden, 1948.
- 7. Goldstein, David L. and Richard Scherrer. "Design and Calibration of a Total Temperature Probe for Use at Supersonic Speeds," National Advisory Committee for Aeronautics Technical Note 1885, Washington, D. C., May, 1949.
8. Werner, Frank D., Robert E. Keppel, and M. A. Bernards. "Design and Performance Studies for Improved Multiple-Shield Total Temperature Probes," Wright Air Development Center Technical Report 53-194, Wright Patterson Air Force Base, Ohio, April, 1954.
- ✓ - 9. Werner, Frank D. and Robert E. Keppel. "Improvements in Multiple-Shielded Gas Temperature Probes," University of Minnesota Institute of Technology Research Report 102, Minneapolis 14, Minnesota, August, 1954.
- L - 10. Winkler, E. M. "Design and Calibration of Stagnation Temperature Probes for Use at High Supersonic Speeds and Elevated Temperature," Journal of Applied Physics, 25:231-232, February, 1954.

11. Winkler, E. M. "Stagnation Temperature Probes for Use at High Supersonic Speeds and Elevated Temperatures," NAVORD Report 3834, United States Naval Ordnance Laboratory, White Oak, Maryland, October, 1954.
12. Werner, Frank D. and Robert E. Keppel. "Development and Tests of Total Temperature Probes," Wright Air Development Center Technical Report 56-613, Wright Patterson Air Force Base, Ohio, July, 1955.
13. Werner, Frank D., Robert E. Keppel, and Laurence D. Huppert. "Characteristics of Several Total Temperature Probes Suitable for Flight Service," University of Minnesota Institute of Technology Research Report 139, Minneapolis 14, Minnesota, January, 1957.
14. Hagins, R. S. "Evaluation of Stagnation-Temperature Measuring Technique in the Sandia 18-inch Hypersonic Wind Tunnel," Sandia Corporation Research Report 66-518, Sandia Laboratory, Albuquerque, New Mexico, October, 1966.
15. Wood, Robert D. "An Experimental Investigation of Hypersonic Stagnation Temperature Probes," Guggenheim Aeronautical Laboratory, California Institute of Technology Hypersonic Research Memorandum No. 50, Pasadena, California, July, 1959.
16. Warshawsky, I. and P. W. Kuhns. "A Review of the Pneumatic-Probe Thermometer," Temperature Its Measurement and Control in Science and Industry, Vol. 3, Part 2, New York: Reinhold Publishing Corporation, 1962, Pp. 573-586.
17. Welshimer, Don E. "The Experimental Application of Sonic-Pneumatic Probe Systems to Temperature Measurements in a Hypersonic Airstream," Aeronautical Research Laboratories 62-364, Wright Patterson Air Force Base, Ohio, June, 1962.
18. Lee, John D. "The Measurement of Velocity and Temperature in a Hypersonic Laminar Boundary Layer," Aeronautical Systems Division Technical Documentary Report 62-914, Wright Patterson Air Force Base, Ohio, December, 1962.
19. Sivells, James C. "Aerodynamics Design and Calibration of the VKF 50-inch Hypersonic Wind Tunnels," Arnold Engineering Development Center TDR-62-230, Arnold Air Force Station, Tennessee, March, 1963.
20. Moffatt, E. M. "Multiple-Shielded High-Temperature Probes," Society of Automotive Engineering Quarterly Transactions, 5-6:567-580, 1951-52.

21. Moffat, Robert J. "Gas Temperature Measurements," Temperature Its Measurements and Control in Science and Industry, Vol. 3, Part 2, New York: Reinhold Publishing Corporation, 1962, Pp. 553-571.
- * 22. Haig, L. B. "Thermocouple Probe Design Method," Society of Automotive Engineering, 68:81-84, August, 1960.
23. Burington, Richard Stinens. Handbook of Mathematical Tables and Formulas. Third edition. Sandusky, Ohio: Handbook Publishers, Inc., 1949.
24. McAdams, W. H. Heat Transmission. Second edition. New York: McGraw-Hill Book Company, 1942.
25. Ames Research Staff. "Equations, Tables, and Charts for Compressible Flow," National Advisory Committee for Aeronautics Report 1135, Washington, D. C., 1953.
26. Liepmann, H. W. and A. Roshko. Elements of Gasdynamics. New York: John Wiley and Sons, Inc., 1962.

DOCUMENT CONTROL DATA - R & D

(Security classification of title, body of abstract and indexing annotation must be entered when the overall report is classified)

1. ORIGINATING ACTIVITY (Corporate author) Arnold Engineering Development Center ARO, Inc., Operating Contractor Arnold Air Force Station, Tennessee		2a. REPORT SECURITY CLASSIFICATION UNCLASSIFIED	
		2b. GROUP N/A	
3. REPORT TITLE DEVELOPMENT OF THERMOCOUPLE-TYPE TOTAL TEMPERATURE PROBES IN THE HYPERSONIC FLOW REGIME			
4. DESCRIPTIVE NOTES (Type of report and inclusive dates) September 1966 to March 1968 - Interim Report			
5. AUTHOR(S) (First name, middle initial, last name) P. J. Bontrager, ARO, Inc.			
6. REPORT DATE January 1969	7a. TOTAL NO. OF PAGES 70	7b. NO. OF REFS 26	
8a. CONTRACT OR GRANT NO. F40600-69-C-0001	9a. ORIGINATOR'S REPORT NUMBER(S) AEDC-TR-69-25		
b. PROJECT NO. 876A	9b. OTHER REPORT NO(S) (Any other numbers that may be assigned this report) N/A		
c. Program Element 65401F			
d. Task G226			
10. DISTRIBUTION STATEMENT This document has been approved for public release and sale; its distribution is unlimited.			
11. SUPPLEMENTARY NOTES Available in DDC		12. SPONSORING MILITARY ACTIVITY Arnold Engineering Development Center, Air Force Systems Command, Arnold Air Force Station, Tennessee	
13. ABSTRACT An experimental study to develop the criterion necessary to construct a miniature shielded thermocouple total temperature probe suitable for application in the hypersonic flow regime. Particular emphasis was given to the effect that internal velocity and thermocouple junction location relative to the shield entrance had on temperature measurements. An error analysis resulting from heat transfer phenomenon was made. The measured total temperature-to-tunnel stilling chamber temperature ratio was correlated in terms of the entrance flow length-to-probe length ratio. Over the range of parameters investigated both the optimum length-to-diameter and the optimum entrance-to-vent area ratios were found to be two. The entrance flow length-to-probe length ratios effectively correlated the data from probes of a given internal diameter.			

14. KEY WORDS	LINK A		LINK B		LINK C	
	ROLE	WT	ROLE	WT	ROLE	WT
probes thermocouples temperature measurement hypersonic flow instruments wind tunnels						